LAWRENCE
LIVERMORE
NATIONAL
LABORATORY

LLNL-JRNL-635880

The Development and Application of NMR Methodologies for the Study of Degradation in Complex Silicones

R. S. Maxwell, J. P. Lewicki, B. P. Mayer, A. Maiti, S. J. Harley

April 30, 2013

Concise Encyclopedia of High Performance Silicones

Disclaimer

The Development and Application of NMR Methodologies for the Study of Degradation in Complex Silicones

Robert S. Maxwell, James Lewicki, Brian P. Mayer, Amitesh Maiti and Stephen J. Harley
Lawrence Livermore National Laboratory
Livermore, CA 94550

Abstract

A broad range of network elastomers based on poly(siloxane) resins are used ubiquitously in aerospace, home and healthcare industries. Accurate predictions of the properties, performance and effective lifetimes of such complex silicone materials are non-trivial due to their inherent structural complexity and physical intractability. Nuclear Magnetic Resonance (NMR) offers perhaps the most effective and comprehensive means of probing the structure and properties of complex silicone materials - from an atomistic to a macro-molecular scale. In this chapter, the wide range of NMR methodologies that may be applied to the study of the structure, dynamics and degradation of silicone based materials are discussed and reviewed. Brief discussions of both common and less frequently utilized NMR approaches will be discussed. An overview of how insights from NMR can be used to gain further insight into structure property relationships and how engineering properties change as a function of degradation mechanisms is also provided.

Table of Contents

Introduction

Typical silicone elastomeric commercial products are complex, multimodal networks with a variety of chemically distinct side groups, crosslink sites, physical entanglements, free chain ends, end-to-end chain lengths, and filler phases that all influence/control the overall network properties (see multiple entries in this volume and **Figure 1**).

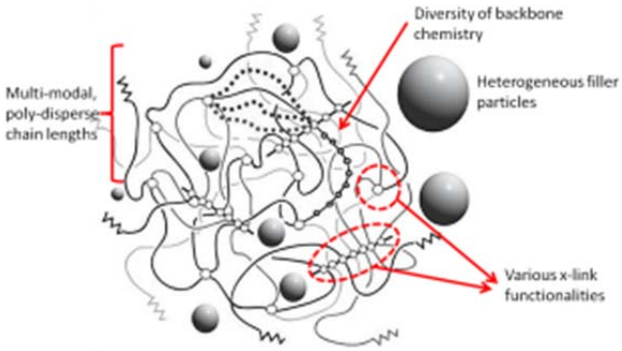

Figure 1. Generalized illustration of the typical network structure of a silicone elastomer material, highlighting the some of the complexities associated with such systems.

These characteristics, however, make characterization of the network structure and how it may change as a function of time, temperature, radiation, stress, etc., difficult to characterize in sufficient detail to make predictions of component performance. This issue is of particular concern since aging of these materials can progress via multiple competing chemical and physical mechanisms that often occur over a broad range of length and time scales, as illustrated in **Figure 2**.

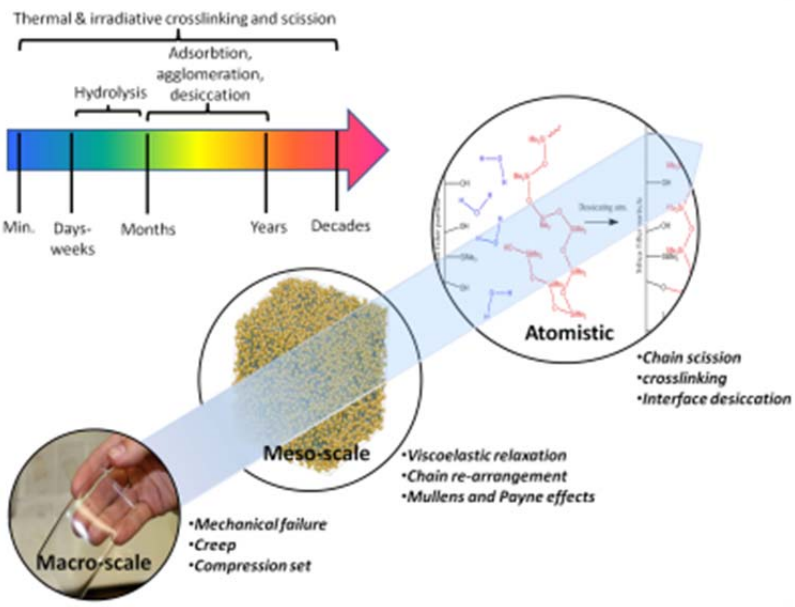

Figure 2. The global properties and dynamic complexities of silicones are a consequence of a range of physical and chemical processes which operate over a broad range of size scales - from the marcoscopic to the atomistic, and an equally broad range of timescales - from minutes to decades.

Additionally, the changes associated with this aging may be subtle, and may not necessarily change linearly – or even exponentially - as a function of time in service.[1-4] Given the well documented difficulties with extrapolation approaches to lifetime estimation, there is a fundamental need to develop and validate strategies employing more sensitive characterization and modeling methodologies to investigate the structural and motional changes that occur in these materials. Ideally, these methods would allow a complete assessment of aging mechanisms such as the monomer content, the number of functional or reacted crosslinking sites, the molecular weight distribution (MWD) between crosslinks, and structure and dynamics at the filler–polymer interface. Methods that can quantify porosity

and free volume and computational methods that provide further physical chemical insight are also needed to connect these observables to engineering properties.

Silicone elastomers are covalently crosslinked networks with an effective infinite molecular weight and are, as such, insoluble and intractable. Consequently the interrogative spectroscopic and imaging methodologies that may be employed to probe such a network structure are almost wholly confined to the solid state. Surface vibrational spectroscopies; attenuation total reflectance Fourier transform infra-red (ATR-FTIR) and resonance Raman spectroscopy can provide broadly averaged chemical information in terms of major functional groups, (see **Figure 3**) however these are limited in sensitivity, penetration depth and may only analyze a surface or physical cross-sectional slice of a material.[5]

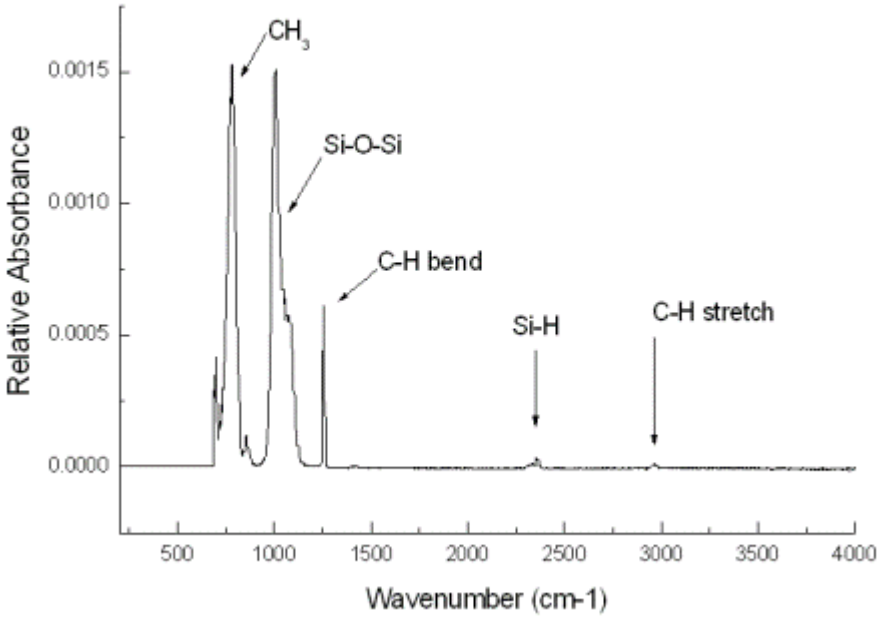

Figure 3. ATR_FTIR analysis of the commercial silicone elastomeric foam -Dow Corning RTV 5370. Although the overall chemical functionalities of the silicone are observable using vibrational spectroscopy they provide only broad average of the

materials structure and provide little information on the network structure and morphology.

Surface imaging techniques such as atomic force microscopy (AFM) and electron microscopy, while able to provide information on physical structure (filler dispersion, phase domain size and distribution) down to a resolutions of 10's of nanometers, yield no direct chemical information on a material. As with the surface spectroscopes, imaging can only access information on a 2-D surface or physical cross-section.[5] As such, AFM and EM are typically employed for purely qualitative assessments of physical structure in silicones. X-ray Computed Tomography (X-ray CT) imaging has the advantage of high resolution in 3-dimensions and has been utilized in the study of mechanical aging and physical structure in engineering silicone foams.[6-8] But X-ray CT provides no information on the chemical speciation of a material, only its physical structure. Light scattering techniques are of little use in the majority of silicones due to their high filler content, however X-ray diffractrometry and neutron scattering techniques can be utilized to probe filler content, dispersion and morphology[9-11] (see **Figure 4**).

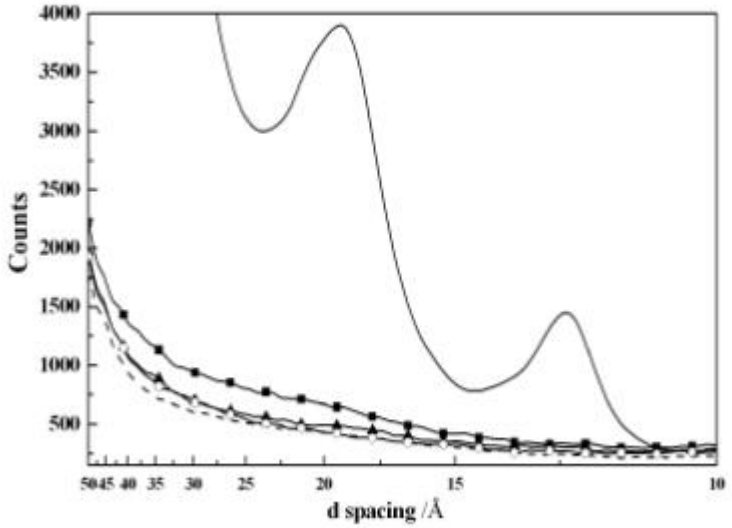

Figure 4. Wide-Angle XRD traces of a series of model siloxane elastomers filled with varying levels of an organically modified nano-clay filler. The solid, dashed, circle, triangle and square lines represent the XRD traces of the clay powder and the elastomer filled with 0-8% nanoclay. The conspicuous lack of any diffraction peaks in the filled elastomers is evidence of the effective 'exfoliation' of the clay filler within the polymer.

Despite the utility of such techniques as probes of the structure and morphologies of secondary phases within silicone systems, they are fundamentally still limited by the fact that they provide no direct quantifiable information on the network architecture of a silicone. It is Nuclear Magnetic Resonance (NMR) that is unique and alone in its ability as a family of techniques to probe the structure and properties of intractable polymeric systems such as silicone engineering elastomers from an atomistic-molecular scale (high resolution chemical shift dependence), in terms of its dynamic physical structure (relaxometry) and at a micro/macroscopic scale (magnetic resonance imaging (MRI)).

In the sections to follow we first review some of the more common uses of "standard" NMR experiments for study of silicone degradation. This is then followed by a review of recently developed capabilities for quantifying the effects of degradation and finally, how this data can be used to develop predictive models of silicone performance.

Applications of NMR for Characterizing Silicones

NMR is a spectroscopic technique based on the application of radio frequency irradiation to nuclear spins held within a static magnetic field. It is often used to obtain information on both the chemical and dynamic nature of various molecular and material classes, including soft polymeric solids. The basics of the field of NMR in both the solution and solid state is well reviewed and, over the last 60 years, NMR methods have shown significant power for characterizing polymeric materials.[12-15] For typical silicone materials, all of the elemental constituents are observable quantitatively and selectively by NMR methods. The most common observed NMR-active nuclei, ^{1}H, ^{13}C, ^{19}F, and ^{29}Si, are easily observable, while ^{17}O and ^{2}H require isotopic enrichment – though this can yield distinct advantages for characterizing response to chemical or physical stress.

All the observable nuclei can provide insight into the chemical speciation through correlation of frequency (quantity) with chemical shift (chemical identity)[12-15] and into the rates and trajectories of motion through measurements of anisotropic interactions such as dipolar and quadrupolar couplings.[12-15] NMR methods have the added benefit of being broadly applicable over a range of phases

of the polymer: from soluble polymer chains and melts to crosslinked elastomers, glasses, and polycrystalline samples. Some of the advantages of NMR for the analysis of silicone polymers are summarized in **Table 1**.

Table 1. Advantages of NMR for analysis of silicone polymer

Solution state methods	**Solid state methods**	**Imaging methods**
Multidimensional, multinuclear experiments for unambiguous structure determination		
Selective observation of speciation through ^{1}H, ^{29}Si, ^{13}C, ^{17}O, and ^{19}F NMR		
Characterization of diffusion rates		
Characterization of dynamics over timescales spanning greater than 10 decades		
High resolution spectra	Non-destructive	
Speciation of networks via solvent swelling (quasi-solution state)	Characterization of response to stress in situ	
N/A	Can be performed in the field in some cases[16-18]	
N/A	Resolution among ^{29}Si environments (silica, siloxane, etc.)	
N/A	Small material quantity required (<1 mg in some cases)	N/A
N/A	Selective detection of crystalline, amorphous, and interfacial domains	N/A
N/A	Quantification of domain sizes	N/A
N/A	Characterization of network structure in crosslinked networks	N/A

Chemical Speciation in the Solution State

Significant work has been reported utilizing solution state ^{1}H, ^{13}C, and ^{29}Si NMR to characterize the structure and chemistry of siloxane based polymer systems.[19] Extensive lists of chemical shifts have been tabulated[19-22] and standard one- and two-dimensional NMR methods such as COSY, HSQC, and HMBC are

routinely used to characterize soluble siloxane polymers of low to moderate molecular weight or their precursors.[19] As will be discussed below, higher dimensional NMR spectra are also now routinely available to the silicone researcher to detect chemical species that are closely related and thus may overlap spectrally in only one or two spectroscopic dimensions. These techniques can be used to characterize chemical degradation in silicone polymers that can be solubilized, particularly when the dominant degradation mechanism is chain scission. In the case of crosslinking reaction, information can be obtained until the gel point, at which point broadening of the NMR spectra may retard the researchers ability to extract structural information. Though as this will be discussed later, this does not constitute an impenetrable barrier and actually leads to what might not, at first, appear to be surprising advantage.

The effects of degradation, however, can still be inferred from tracking changes in the soluble chemical species produced by the various degradation mechanisms. Stephens et al., for example used ^{1}H solution state NMR of extracts from the Dow Corning product RTV5370 exposed to ionizing radiation to detect oligomeric siloxane residues.[23] And in recent years, solution state NMR has been increasingly used to understand the mechanisms of silicone medical implant degradation during service in biological systems, as illustrated in **Figure 5**.

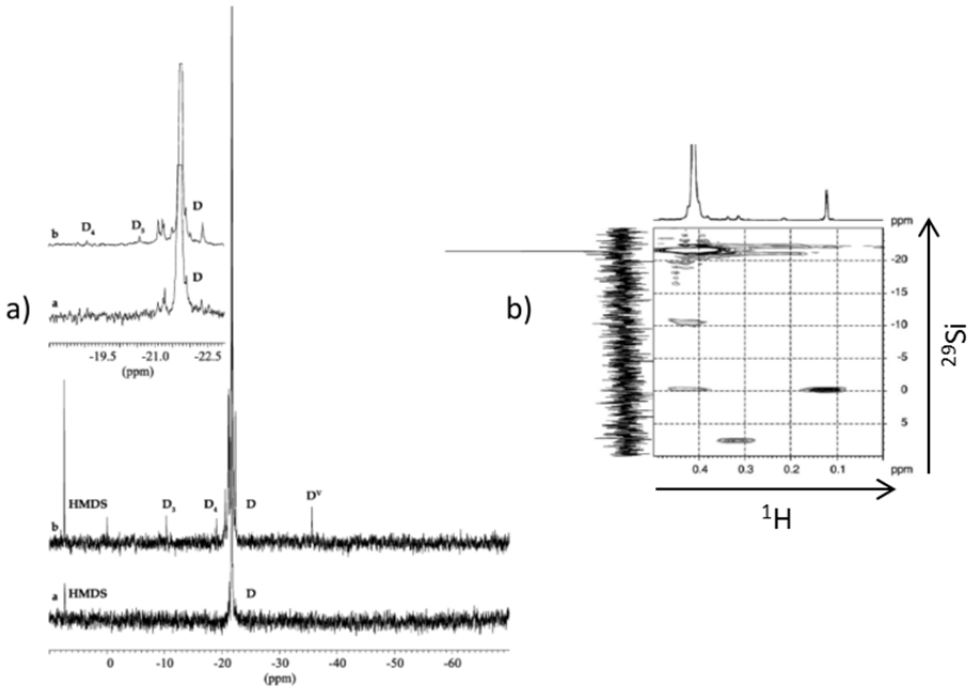

Figure 5. Solution-state ^{29}Si NMR analysis of silicone breast implant materials can be utilized to characterize chemical species associated with degradation. (a) The chemical shifts measured in ^{29}Si NMR allow one to correlate distinct NMR signals with changes in specific chemical functionalities present in the system *i.e.* cyclic oligomers denoted 'D_{n-x}' in the figure. (b) 2-dimensional ^{29}Si-^{1}H HSQC heteronuclear correlation experiments dramatically increases sensitivity of the ^{29}Si NMR spectrum (as illustrated by the cross-peaks indicating bonding between ^{1}H and ^{29}Si resonances that are not observable in the direct ^{29}Si NMR spectrum (vertical spectrum)[24]

In the study reported by Birkfield,[24] ^{29}Si NMR has been used to detect changes in the implant constituents while ^{1}H and ^{13}C NMR have been used to measure the chemical species that have managed to migrate to neighboring tissue.[24] Standard 2D NMR correlation experiments have also been utilized to gain increased structural insight and increased sensitivity (see **Figure 5**). Results such as these can then be used to inform toxicological assessments and to estimate implant lifetime.

Chemical Speciation in Insoluble Networks – NMR of the Swollen State

Given the rapid motion occurring in most silicone melts, spectral broadening is relatively limited (see **Figure 6**) compared to what is usually observed in organic polymeric materials below their T_g where NMR resonances can be effectively broadened into the baseline.[12]

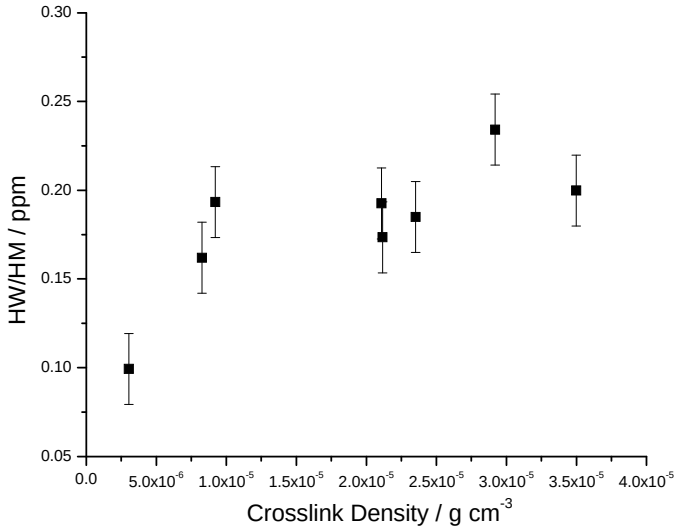

Figure 6. ^{1}H peak half-width/half-max (HW/HM) (of the comparatively narrow PDMS methyl proton peak at ~0 ppm.) vs. crosslink density for a series of end-linked silicone elastomers, over a range of crosslink densities of ~3.0 x 10^{-6}-3.5 x 10^{-5} mol. cm^{-3}. While some line broadening is evident, even at the highest x-link densities, the methyl proton peaks are still considered narrow.

Given the relatively narrow spectra obtained for silicones well above T_g, chemical speciation can be detected in solid materials without further adjustment of the NMR spectrometer over what was utilized in the typical solution state experiment. However, swelling in a good solvent can provide additional degrees of motional freedom and increase resolution. This can be particularly valuable when detecting the non-^{1}H NMR active nuclei. Recently, Alam, et al., for example, reported

the use of isotopically enriched $^{17}O_2$ and $H_2{}^{17}O$ to characterize the effect of oxygenation and hydrolysis reactions on the chemical structure of irradiated and thermally degraded silicones.[25-27] These approaches are elegant in that the only spectroscopically observable ^{17}O originates from chemical reactions of the labeled species with the polymer network – allowing, for example, the direct quantification of the formation of silanol sites due to chain scission or formation of silico-ether linkages due to chain scission followed by re-condensation and elimination of water (see **Figure 7**).

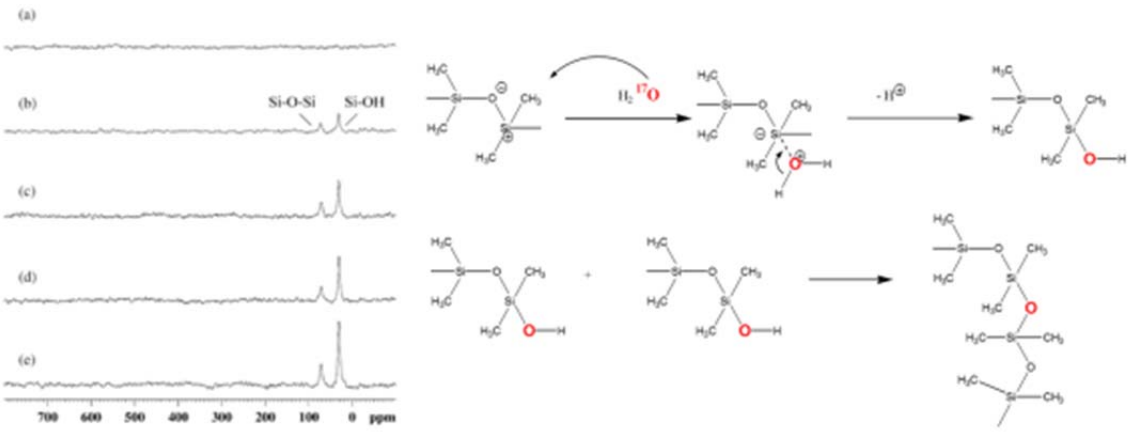

Figure 7. ^{17}O labeled O_2 or H_2O has been used to monitor selectively the extent of oxidation and hydrolysis reactions occurring during exposure to ionizing radiation through detection of the ^{17}O NMR spectrum. No resonances are observed in the pristine material due to the very low natural abundance of ^{17}O in the unaged polymer network[26]

Similar experimental protocols have shown how the use of reactive fluorination agents can produce unique ^{19}F NMR signals due to reaction with silanol, alcohol, or other reactive sites due to degradation.[28]

Direct Detection of Chemical Speciation Changes in the Solid State

In the solid state, NMR spectra are typically much broader than typically obtained in solution state NMR. This is due the low native mobility of condensed phase polymer chains leading to anisotropic magnetic interactions which broaden the NMR resonances (i.e. the presence of dipolar interactions between nuclear spins, quadrupolar interactions between isotopes with nuclear spins greater than ½ (^{17}O and ^{2}H, for example) and electric field gradients, or chemical shift anisotropies).[29-30] The most commonly used approaches to remove this broadening utilize magic angle spinning (MAS) to increase spectral resolution. MAS involves mechanical rotation of the sample at kilohertz frequencies. This spinning, if fast enough, can average out the effects of various interactions (homonuclear dipolar couplings) that would otherwise severely broaden the NMR line-shape.[12-14] MAS NMR has been frequently and effectively exploited for obtaining direct, high resolution ^{1}H, ^{13}C, ^{29}Si, and ^{17}O NMR spectra of silicones, including quantifying polymer, filler, and chemical functionalization such as silation.[13,19,31] Shown for example in **Figure 8** is a solid-state direct ^{29}Si MAS spectrum of a silica filled, engineering silicone elastomer.

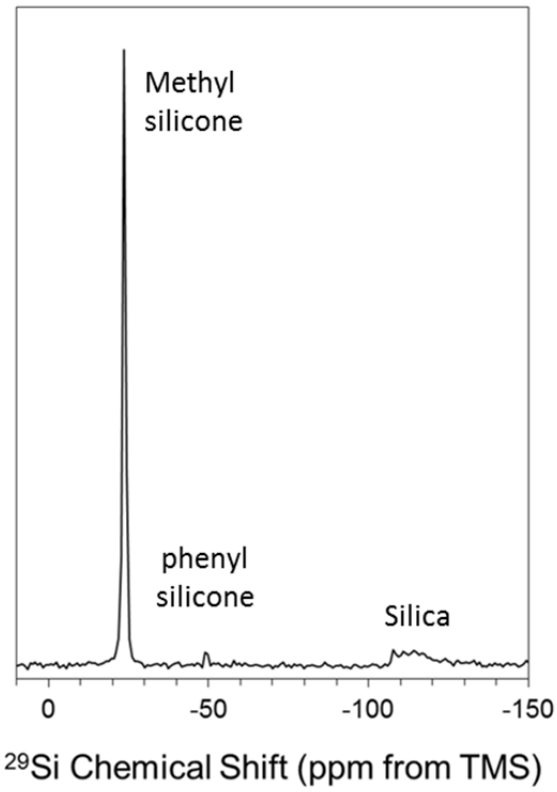

Figure 8. Solid state MAS ^{29}Si spectra of a silicone-based engineering elastomer, M9787. This is a "direct" ^{29}Si polarization; all silicon nuclei are observed and can be quantified directly, albeit with limited sensitivity

Labouriau, et al. utilized ^{29}Si MAS NMR to detect changes in the distribution of Di-siloxane/Tri-siloxane/and Quartenary siloxane speciation with age.[32] Lewicki, et al. similarly used ^{1}H MAS to quantify changes in silane and silanol species during network formation.[33] Extending the approach developed by Alam, et al.[25] Patel detected re-arrangement of the silicone network and the formation of oligomeric degradation products through the use of ^{17}O MAS NMR.[34] As mentioned previously, a particularly useful technique reported by Assink et al.[28] is based on a method first reported by Mueller et al.,[35] where fluorinated silating agents can be used to

quantify at extremely low levels of detection degradation induced species formed in both insoluble and soluble polymer networks and at the filler surface.

Qualitative Characterization of Changes in Network Structure through Changes in NMR Relaxation Phenomena in the Solid State

Researchers have been utilizing nuclear spin relaxation based methods (sometimes broadly referred as "relaxometry"[12]) to characterize both linear, melt-state siloxane polymers and polymeric material comprising solid elastomers for more than four decades.[12,36-40] It was observed early on that there were numerous correlations between the broad spectrum of segmental motions in silicone elastomers to a number of NMR relaxation times, including the transverse relaxation times (T_2), spin-lattice relaxation times (T_1), and the spin-lattice relaxation time in the rotating frame ($T_{1\rho}$). Some of the first reports were the classic papers by Charlesby measuring relaxation times of short chain silicone polymers exposed to increasing doses of gamma irradiation.[41-44] Since these initial studies, there has been much research in understanding the fundamental physics governing the relationship between various relaxation times and network structure in both elastomer and molten polymer systems using existing knowledge of both their mechanical behavior and theories of polymer physics.[12,40,45-52] In fact, over the years, the transverse relaxation time (T_2), most conveniently measured using Hahn or Carr Purrcell Meibloom Gill (CPMG) Spin-echoes, have become a standard indirect measure of crosslink density changes in silicones. An example is given in **Figure 9** where the measurement of the transverse relaxation time (T_2) for an engineering silicone has been directly correlated with crosslink density changes brought about

by irradiative aging. These simple to implement spin-echo experiments can also directly detect the fraction of network versus sol chains and have been routinely used to obtain the chain scission vs. crosslinking yields for irradiated silicones through the Charelsby-Pinner analysis.[13,53] Such comparatively simple solid state methodologies can therefore be utilized as an effective probe of the segmental dynamics, local order and even the global architecture of complex silicone systems.[54]

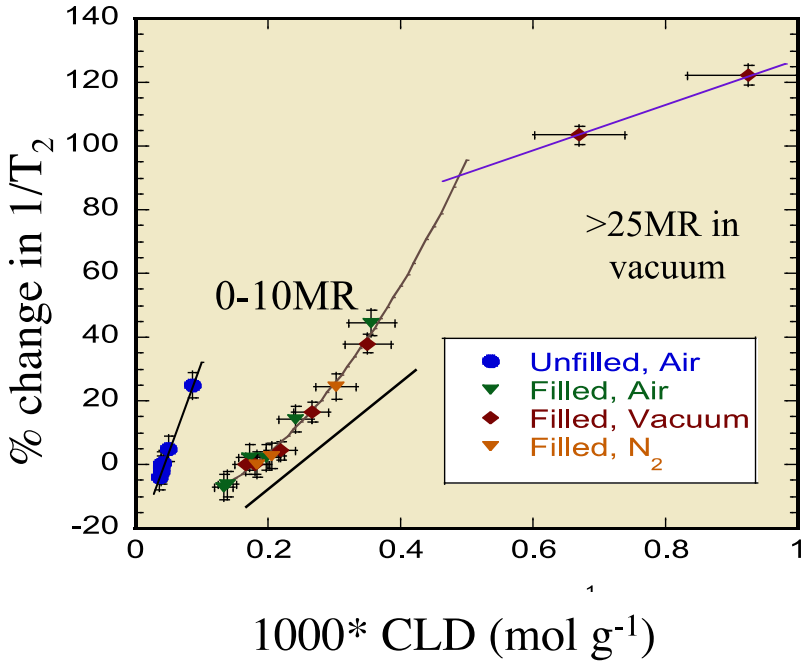

Figure 9. Correlation between transverse relaxation times (T_2) and bulk average crosslink density of a bimodal silicone network, both filled and unfilled, exposed to gamma-radiation. In general, over moderate ranges of changes in crosslink density a linear correlation is usually found in a similar family of silicones. Over large ranges of doses (see break between 10MR and 25 MR), non-linearities can be observed, most likely due to changes in aging mechanisms.

This sensitivity is due to the fact that in addition to speciation obtainable via chemical shifts, NMR spectra also reflect, for example, the through space magnetic interaction between nuclear spins. These are the same phenomena that serve to broaden the NMR spectrum in the solid state discussed above. The dipolar interaction, in particular, is dependent on both the distance between interacting nuclei and the orientation of the internuclear vector with respect to the applied magnetic field. In the presence of motion, both the distance and the orientation become time dependent and can have dramatic effect on both solution- and solid-state NMR spectra.[12] For typical silicone elastomers, low glass transition temperatures (T_g; for silicone elastomers typically well below room temperature) and an innately high degree of backbone flexibility result in small dipolar coupling magnitudes (vis-à-vis other elastomeric materials), which lead to narrow NMR resonances (peaks) even in solid materials.

These dipolar couplings, however, are not zero as observed in typical solution state NMR spectra of small molecules. This reduced, non-zero, dipolar coupling is referred to as the residual dipolar coupling (RDC, $<\Omega_d>$, or D_{res}) and is understood to be the result of topological constraints (cross-links and physical entanglements) that interfere with fast chain reorientations on the NMR timescale that otherwise would be expected to average homonuclear dipolar couplings to zero. There is also a time dependent fluctuation in the residual dipolar coupling $\delta<\Omega_d>$ that can be measured by particular NMR experiments.[55] These residual dipolar couplings, in fact, have been shown to be quite sensitive to dynamic and morphological changes[53,56-66], can be measured with a number of experimental

methods (as illustrated in **Figure 10**) and can be directly correlated with structural parameters such as the net crosslink density and to measurements of bulk physical properties such as the Young's and bulk modulus.[67]

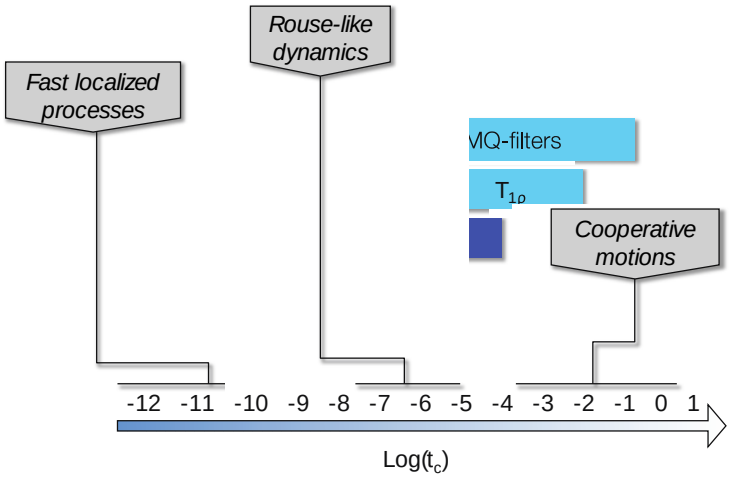

Figure 10. Illustration of the broad range of timescales over which the various motional NMR observables, relevant to polymeric systems occur and the relaxometry techniques sensitive to those processes.

As a result of such studies, it is now both convenient, fairly straightforward and relatively common to use a combination of relaxation based methods and high resolution NMR spectral methods to obtain chemical insight into assessments of network structure of silicone materials both in formulation and degradation studies, an example of which is shown in **Figure 11**.

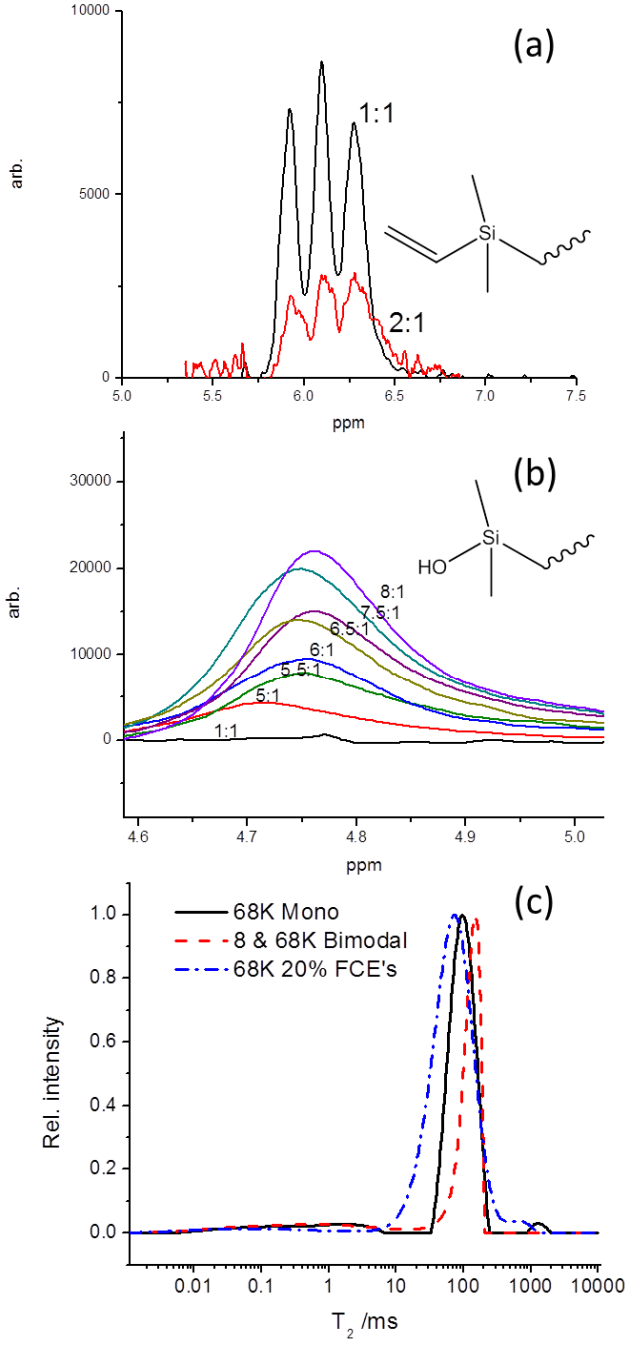

Figure 11. Solid state ^{1}H MAS and T_2 relaxometry can provide structural information on a silicone network. (a-b) ^{1}H MAS allows direct observation and quantification of residual levels of reactive side groups and crosslink moieties in a solid elastomer series formulated with varying ratios of vinyl to silane groups from 1:1 to 8:1 Si-H to vinyl. Note that it is the hydrolyzed silanol we detect. (c) Direct

measurement of the distribution of T_2 can be measured and correlated to network modality and structure (e.g. changes in crosslink density, modality and free chain ends) in (c) we observe that a 68K Da monomodal network, an 8 and 68 KDa bimodal system and a 68 KDa monomial network with 20 mol. % free chain ends each have a distinct T_2 response.

Highlights of Recent Advances in NMR Methodology

Over the last 15 years, several advanced experimental NMR methodologies, in both the solution and the solid state, have been developed for the analysis of complex silicone systems, their structures, and the mechanisms of aging and degradation. As discussed above, chemical shift data and relaxation phenomena have been exploited for decades to gain insight into e.g. the identity of crosslinks in PDMS networks, the dynamical behavior of melt-state polymer chains, correlations among physical and chemical properties of polymeric material and a variety of NMR observables, etc. While these strategies have proven fruitful in the past, much work has been performed in the development and application of advanced NMR experiments that can yield even deeper insight into not only silicone-based materials but a wide variety of other soft solids. Below we highlight a few of the recent advances in NMR methodological development.

High resolution "n" Dimensional-NMR for Advanced Speciation

While multinuclear chemical shift information can in principle yield a wealth of information on chemical species present in a given sample, the spectra of condensed-phase material can be plagued by large linewidths - even in soluble polymers - due to overlap of chemical shifts of structurally similar species, such as a

single moiety present in multiple environments. This is particularly problematic for ^{1}H spectra where broad peaks coupled with a relatively small chemical shift dispersion (ca. 10 ppm) often results in complicated, overlapping peaks that are difficult, if not impossible, to de-convolve from typical one dimensional spectra.

To tackle the above issues, multidimensional NMR experiments have been developed that help resolve overlapping peaks by separating them based on, for example, the chemical shifts of a heteronucleus.[68-70] In the case of many compounds, it is often desirable, for example, to perform proton-carbon heteronuclear correlation experiments such as 2-D $^{1}H/^{13}C$ or $^{1}H/^{29}Si$ HSQC or HMQC experiments to gain increased insight into chemical bonding arrangements.[19,68] In silicones, separating ^{1}H NMR spectra by the bonding to ^{13}C or ^{29}Si (often methyl groups) can be insufficient. As a result, increasing application of three-dimensional NMR spectroscopy to the characterization of silicone materials has occurred in the last decade. Rinaldi et al.,[71] for example, employed $^{1}H/^{13}C/^{29}Si$ NMR combined with pulsed field gradients to characterize and completely assign resonances for a small PDMS oligomers. Such an application is shown in **Figure 12**.

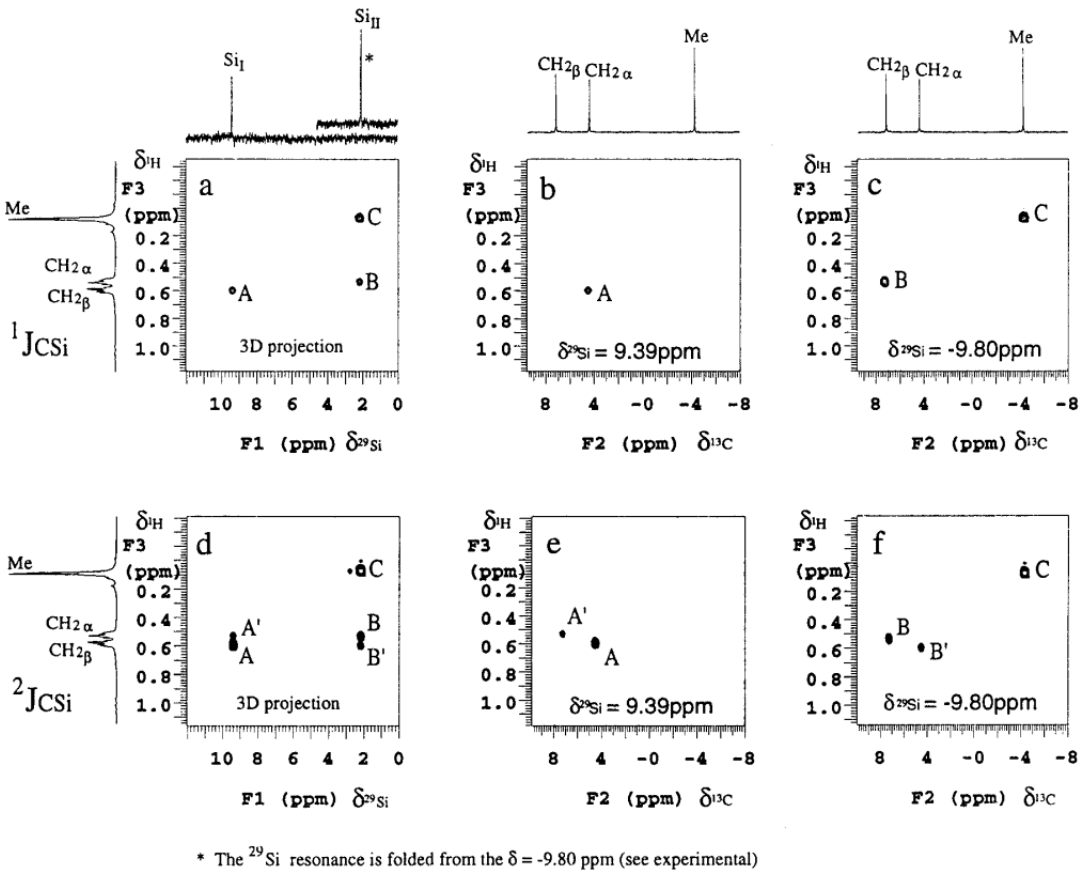

* The ^{29}Si resonance is folded from the δ = -9.80 ppm (see experimental)

Figure 12. ^{1}H/^{13}C/^{29}Si 3D NMR spectra of a first generation carbo-silicone dendrimer. (a)3D f_1f_3 projection of the one-bond C-Si ^{1}H/^{13}C/^{29}Si 3D NMR spectrum; (b-c) f_2f_3 slices at different ^{29}Si chemical shifts from the one-bond C-Si ^{1}H/^{13}C/^{29}Si 3-D NMR spectrum: (b) f_2f_3 slice at δ_{29Si} = 9.39 and (c) f_2f_3 slice at δ_{29Si} = -9.80; (d) 3-D f_1f_3 projection of the multiple-bond C-Si ^{1}H/^{13}C/+Si 3D NMR spectrum; (e-f) f_2f_3 slices at different ^{29}Si chemical shifts from the two-bond C-Si ^{1}H/^{13}C/^{29}Si 3D NMR spectrum; (e) f_2f_3 slice at δ_{29Si} = 9.39 and (f) f_2f_3 slice at δ_{29Si} = -9.80.

Again, the relatively large native ^{29}Si chemical shift range allows for the removal of significant spectral overlap that would otherwise be present in the one dimensional proton or carbon spectra since the oligomer contains primarily methyl groups. Another example from Rinaldi et al.[72] was the structural identification of complex carbo-silane dendrimers though the use of a single multi-dimensional NMR technique - which enabled the selective detection of signals from one-bond and

two-bond connectivities among ^{1}H atoms coupled to both ^{13}C and ^{29}Si at natural abundance. The richness of spectral dispersion and the molecular connectivity information present in such 3-D NMR spectra enable the provision of accurate resonance assignments and definitive proof of structure in highly complex silicone based systems. Extension of these methodologies to include ^{19}F to yield increased insight into fluoro-silicones are also now routinely possible with modern spectrometers.[28]

Cross Polarization Methods for Characterizing Filler Interactions

In the solid state, the information hidden in the line-widths (such as motional rates or spatial proximity), is generally lost in MAS experiments. Many advanced techniques, however, have been developed in the recent decades to obtain high resolution NMR spectra of solid materials while retaining dynamic information so that information on chemical speciation and chain/monomer motial rates and trajectories can be obtained in one multidimensional NMR experiment.[12] Solid-state NMR experiments that can detect spatial proximity of NMR active spins from one phase to another through dipolar couplings are increasingly being used to characterize polymer-surface interactions in silicones through exploiting through-space interaction of proximate NMR active nuclei (such as protons of silanol groups on the silica surface and polymer silicon atoms). Variable contact time, cross polarization MAS experiments have been used to gain such information in a wide variety of silicone and other elastomeric materials.[73-76]

Cross polarization (CP), at its most basic, consists of a transferal of magnetization from an abundant, sensitive nucleus (proton, for example) to a less

abundant "X" spin (carbon, silicon). This transferal results in a much stronger X magnetization than that obtained through direct excitation and allows for faster repetition times since the experiment depends only on the spin lattice relaxation time of the proton (generally shorter than that of the X nucleus). Therefore, experiments can be conducted in a fraction of the time it would take to direct detect silicon or carbon. More importantly, however, is that because this magnetization is transferred over relatively short distances, only species in intimate contact with protons will be cross polarized. In this way, polymer/surface interactions can be probed quite specifically and sensitively. This is dramatically illustrated in the CPMAS spectrum (**Figure 13**) of the same filled silicone elastomer shown in the MAS only spectrum in **Figure 8**. In a standard direct polarized MAS spectrum, these observed bound resonances are unobservable since the majority of ^{29}Si spins observed belong to the mobile chains in the network that are not surface bound or associated (compare **Figure 13 and 8**).

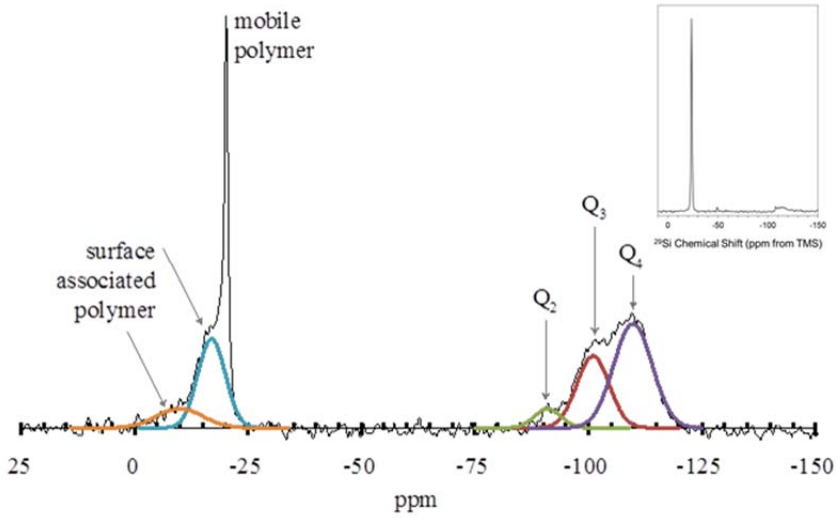

Figure 13. $^{29}Si\{^{1}H\}$ CPMAS spectrum of the same filled engineering silicone as in **Figure 8**. Note the dramatic increase in the siloxane resonances from the inorganic

filler near -100ppm and the surface adsorbed chains near -12 and -20 ppm and the decreased strength of the resonance from the mobile silicone chains at -21ppm compared to the ^{29}Si MAS spectrum shown in **Figure 8** and the inset here.

Following the pioneering work by Maciel in the 1980's which utilized ^{29}Si CPMAS methods to characterize the surface attachment of silation agents to high surface area silicas,[77-79] these methods have become somewhat standard method for characterizing inorganic/organic hybrid materials with a significant amount of silica. Because of the rapid mobility of the PDMS network chains interferes with the polarization transfer mechanism, obtaining high quality CPMAS spectrum can be difficult in low filled composites and has been somewhat underutilized. The work of Aramata and Igarashi[80] represents one of the first uses of CP-MAS to investigate the silica-siloxane interface in a silicone elastomer. The research exploited this technique to detect the silica surface-bound ^{1}H PDMS species. Their presence was concluded based on weak but detectable silicone ^{29}Si peaks that were shifted and broad compared to the bulk siloxane resonance. This shift and broadening were interpreted as resulting from the electronic environment at the silica surface and in the restricted mobility of the chains associated with the filler interface, respectively.

For example, Milanesi et al.[81] used CP-MAS to investigate films of tri-functional siloxane containing titania nanoparticles. The research focused on assessing the modes of attachment of the siloxane polymer to the TiO_2 surface and more specifically the structure of the chemisorbed, hydrophobic polymer layer. Using ^{29}Si chemical shifts the authors were able to derive specific structures (mono-, di-, and tri-functionalized) of surface-attached siloxane chains, as illustrated in **Figure 14**.

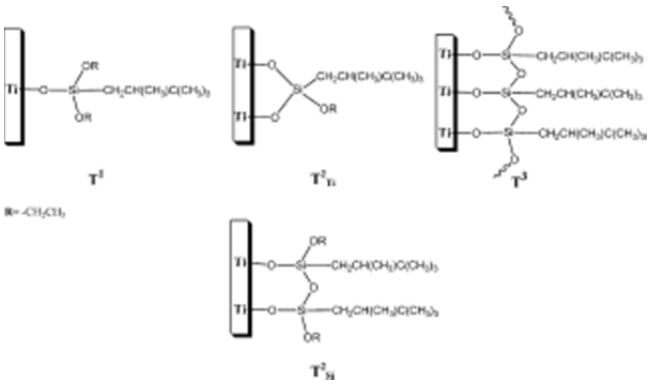

Figure 14. Proposed structures of titania-chemisorbed siloxane chains derived from $^{29}Si/^{1}H$ CP-NMS experiments in Milanesi et al.[81] It was observed that the various T_2 structures (di-functionalized chains) were the dominant reaction product.

A similar study was also conducted on a filler-reinforced siloxane elastomer by Luliucci et al. in 2006.[82] The group used a combination of $^{1}H/^{29}Si$ CP-MAS and 2D HETCOR spectra to investigate the nature of the curing process of silica-filled, PDMS-based DC745 (see **Figure 15**) and concluded that the observed changes in the NMR observables were due to dehydration of the silica surface during the curing process.

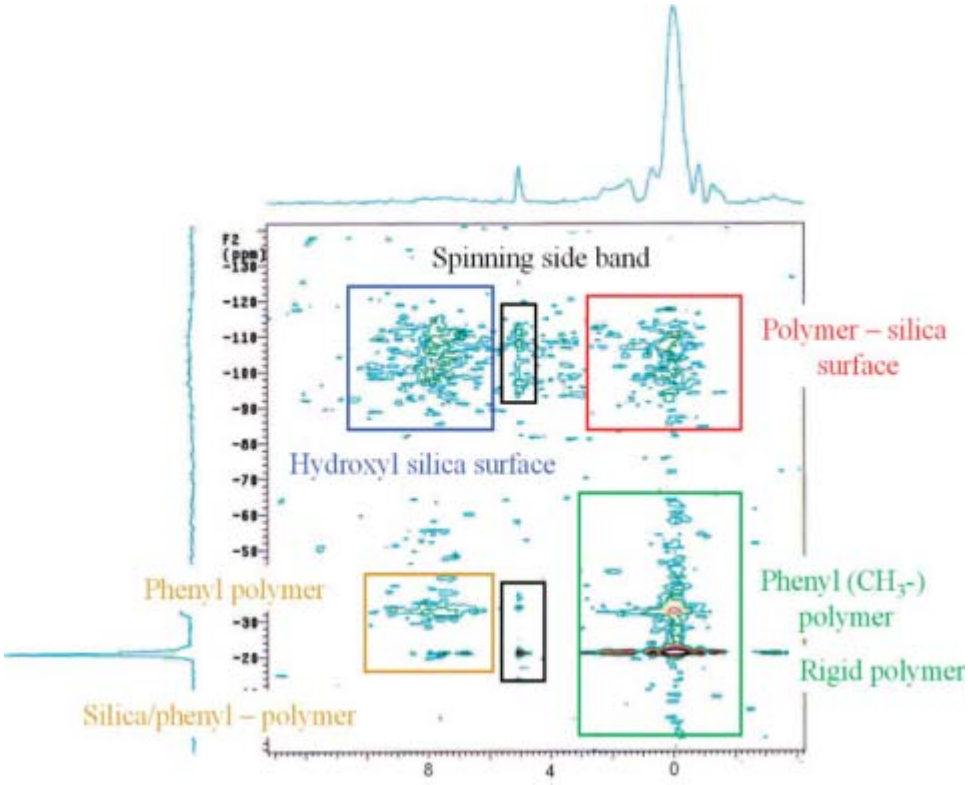

Figure 15. The results of the Luliucci et al. 2006 2D Heteronuclear Correlation (HetCOR) study of an aged silicone engineering elastomer Dow Corning DC745.[82] the results show increased coupling (thus decreased internuclear distance) between polymer and silica surface. ^{1}H chemical shifts are horizontal while the ^{29}Si shift is vertical.

The detection and quantification of multiple quantum coherences in spinning and static samples have also been utilized to detect changes in surface interactions.[83-86]

Advanced Relaxometry Methods

In addition to the more simplistic relaxometric techniques outlined briefly above, there have been developed more elegant approaches to relaxometry that yield more robust, specific data. Consider spin-spin (transverse, T_2) relaxation. This process amounts to the de-coherence of transverse magnetization, which results

from a number of complex processes, many in effect simultaneously: dipolar interactions, chemical shift anisotropy, quadrupolar interactions, thermal motion, etc.

For example, decay rates of spin-echos used to measure T_2's can be affected by the natural molecular diffusion processes that occur in polymer systems.[12] Diffusion of spins through magnetic field gradients prevents the refocusing of the precessing magnetization that occurs in the spin-echo experiments and adds an additional decay mechanism. This has been used frequently to quantify diffusion constants when known, quantified, external gradients are applied.[16-17,87-88] Field gradients, however, can also exist within the polymer network due to susceptibility gradients due to voids and filler particles. Silicone polymers, as mentioned, are generally well above their glass transition temperature at ambient conditions and thus they are characterized by significant amount of motion. As polymer chains move through these naturally occurring gradients, they will lose coherence and an additional decay term occurs in the spin-echo decay of ^{1}H NMR. Of interest to degradation studies, one can thus measure changes in void structure and polymer-filler interactions through changes in the decay curves. As illustrated in **Figure 16**, this has been done in both silicone and other elastomers subject to tensile stress.[52,89] The largest scale MD simulations done to date on filled silicone systems have supported previous experimental studies that the void creation is hindered by filler incorporation, but has further suggested that the cavitation formed, preferentially forms near the filler surface.[90]

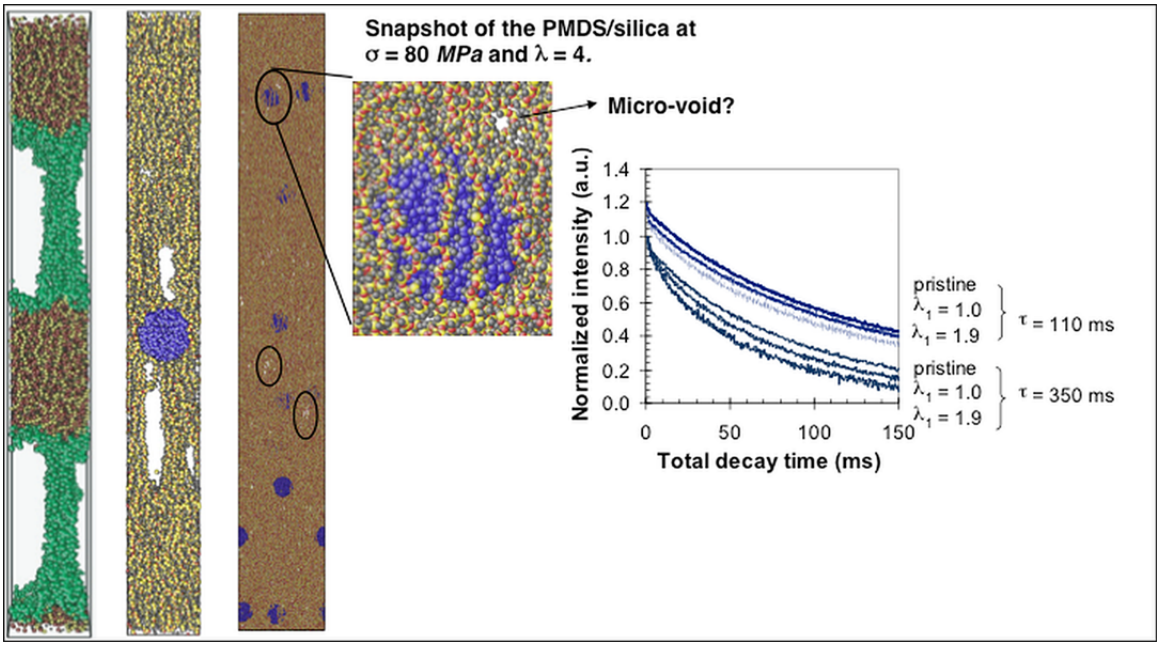

Figure 16. Left: MD simulations of filled silicone systems subject to tensile strain (here lamba=2.0) as a function of filler content showing that cavitation occurs to a larger extent in unfilled networks and that in filled systems, cavitation seems to occur preferentially near the filler surface. MD simulations also allowed the identification of chains that are preferentially ordered along the strain axis (monomers colored green). Right: increased presence of cavitation detected by Carr-Purcell-Meibloom-Gill (CPMG) spin echo NMR experiments on filled networks subject to ionizing radiation while under tensile strain.

In many instances it is important to measure only the effects of a given interaction, and in the case of siloxanes, the phenomenon of most interest is the inter-proton dipolar interaction. For a typical melt state silicone, the measured residual dipolar interaction (see above) is small due to the innately large degree of chain flexibility. The melt's spin-spin relaxation constant, T_2, is corresponding large relative to other polymers in their melt state. However, in more complicated systems like a silicone/silica mixture or a filled engineering elastomer, surface-adsorbed or covalently bound chains are much less mobile. The restricted dynamics of these chains result in an increase of the residual dipolar coupling interaction. In some extreme cases where polymer chains become so rigid as to appear glassy or

even semi-crystalline, the NMR signal may decay so quickly that no information can be obtained.

To address the issue of rigid polymer components, various researchers have turned to "time reversing" strategies that, in a very simplified sense, "restore" the system's memory of magnetization "lost" to strong dipolar interactions. One common strategy is to employ the Magic Sandwich Echo (MSE), which consists of a sequence of sandwiches pulses whose aim is to recover magnetization that would otherwise have been lost in e.g. the spectrometer dead time (lag time between desired and actual detection due to imperfect electronics). Demco et al.[83] employed the MSE early on to determine residual dipolar couplings in natural rubbers. Their "accordion" MSE was able to extract these parameters without obfuscating contributions such as inhomogeneous spin interactions and T_2 relaxation. The MSE has been used to great effect in the work of Papon et al.[56] to determine accurately the fraction of immobilized, silica surface-associated polymer in a model poly(ethyl acrylate) elastomer. Of particular importance is their use of low-field, static *permanent* magnets that result in low-cost, potentially portable measurements with no sacrifice in data quality and reliability.[91-95]

An alternative approach to obtaining information on polymer dynamics and network structure was developed by Ball, Callaghan, and Samulski and called the β function. This experiment amounts to a clever combination of various echoes (both Hahn and solid) like the type used to obtain T_2 decay curves and has been employed to probe inter-proton dipolar interactions. To explain the resultant data, a simple dynamical correlation function was introduced that depended only on the

strength of the RDC and a measure of the tube disengagement time. Values extracted from data on PDMS melts were shown to be consistent with those derived via other methods.[59] These treatments were then extended to polymer networks in both unstrained and strained states.[60] Of particular interest are data from stretched natural rubber, as the experiments were able to detect clearly the microscopic conformational order induced by the macroscopic deformations.

A similar approach to β decay in that it too relies on a combination of echoes is referred to as the dipolar correlation effect (DCE). This technique relies on a ratio of the stimulated and Hahn echoes and has also been applied to the study of silicone materials. Notably, the DCE has been invoked to study the aging of a filled silicone upon exposure to ionizing radiation.[55] These data yielded direct evidence of surface-adsorbed species and shown the fraction of these chains to change as a function of radiation exposure.

Quadrupolar "witness" nuclei

Deuterium (^{2}H) NMR has been applied to extract information on order present in silicone/elastomeric materials.[62,96-99] Many techniques that are used on proton nuclei can also be fully applied to their quadrupolar counterparts. In these studies, order (typically in strained samples) has been detected via the use of deuterated "reporter" or "witness" molecules. These molecules are typical small oligomeric siloxane materials whose ^{2}H NMR spectra may yield splitting patterns due to anisotropies of the quadrupolar interaction that are interpreted as direct evidence of local order in these elastomeric materials. Sotta et al.[62] employed end-deuterated siloxane-based oligomers to demonstrate the existence of short-range

orientational coupling between network chains upon uniaxial deformation of the material.

Other researchers have adopted different strategies with regards to incorporating deuterium nuclei into silicone systems of interest. Deloche and Samulski[100] used a per-deuterated swelling agent to glean information on the orientational order generated by uniaxial deformation. The researchers likened this order to nematic-like interactions over short distances. In a more recent study, Sotta[98] described in detail a large number of ^{2}H-based experiments and demonstrated that a number of NMR observables correlated quite strongly with the properties of elastically effective network chains. The research also highlighted the presence of and differences between dangling (elastically ineffective) chains and those chains that were part of the permanent network of the elastomer. All these quadrupolar strategies have the potential to yield insight into network material that has been modified by a variety of "destructive" factors, though as of this time, little to no research has been published on such cases.

Multiple Quantum NMR

Very recently advanced Multiple Quantum (MQ) NMR approaches have been developed which provide highly sophisticated characterization of both melt state polymers and soft, elastomeric material. They have given researchers tools to assess the MWD of crosslinked network chains and, in combinations with other methods, have improved our ability to quantify the changes occurring at the polymer-filler interface and have provided key insights into the stress heterogeneities in strained components.

MQ-NMR allows for the quantification of dipolar couplings originating between proton nuclei on polymer chains that are under the dynamical and topological influence of various constraints, which prevent the complete motional averaging of the homonuclear dipolar interaction (see **Figure 17**).

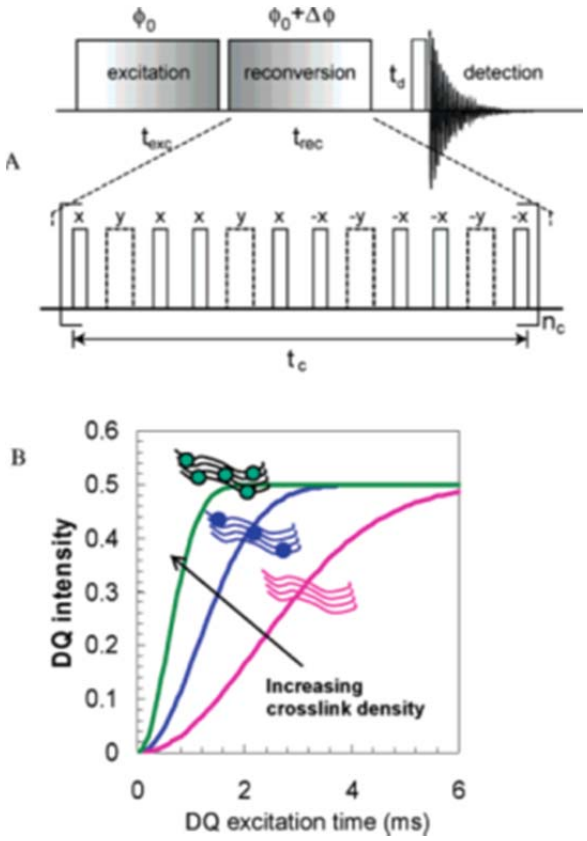

Figure 17 (A) The MQ NMR pulse sequence – the number of pulse-trains (n_c) may be incremented to generate a 'growth curve'. (B) A series of generated MQ growth curves as a function of crosslink density for an elastomer system. The rate of increase in DQ intensity (the DQ build-up time) can be related to the level of constraint within the material.

In MQ-NMR motional dynamics are parameterized by one or, more commonly, a distribution of residual dipolar coupling values, which represent the time- and ensemble-averaged interaction strength between two protons along the chain length. It is important to note that while the majority of the alternative techniques outlined above also rely on this phenomenon, the data resulting from the

MQ-NMR experiments pioneered by Saalwächter and coworkers[63] can be analyzed in a model free way with no assumptions about various motional limits, functional forms of dynamical correlation functions, etc.

The *residual* dipolar coupling magnitude, D_{res}, can be expressed generally through the simple relation,[101]

$$\frac{D_{res}}{D_{stat}} = \frac{3}{5}\frac{r^2}{N}\langle P_2(\cos\alpha)\rangle \qquad \textbf{(Equation 1.1)}$$

which relates the parameter mathematically to the number of effective statistical segments between constraints, N. In the above expression D_{stat} is the static dipolar coupling constant (taken to be 8.9 kHz for rapidly rotating methyl groups as is that case for PDMS), r^2 (generally assumed to be 1 for unstrained samples) is the squared end-to-end vector normalized by its average, melt state value, and $\langle P_2(\cos\alpha)\rangle$ is the time-averaged second order Legendre polynomial of the cosine of α, the angle between the Si-C vector at the chain backbone. This term takes into account rapid, intrasegmental motions; and because the angle α is ca. 90° on average, the value is therefore generally taken to be ½. This equation expressed the anisotropy of the proton-proton dipolar interaction resulting from the non-zero correlation between semi-local segmental motion and the chain end-to-end vector and can be used practically to extract information on both average values and distributions of chain lengths for melt state polymers and networks alike (see below).

The MQ-NMR experiment consists of three main parts. First magnetization is converted (or excited) into a state governed by a dipolar double quantum (DQ) Hamiltonian. This spin state reflects correlated, two-spin interactions that can be exploited to yield information about the strength of the dipolar interaction given that those are two-body in nature as well. The second phase of the pulse sequence is referred to as "reconversion" and both ensures that nearly pure DQ coherences are selected and prepares the magnetization to be detected, as DQ coherences cannot be directly observed. In the final phase the magnetization is read out via a single pulse and detected.

One of the main aims of the MQ-NMR experiment is to obtain data that reflects exclusively structure while removing the effects of dynamics. A conventional NMR signal or spin echo decay is a combination of both structure and dynamics, as discussed previously[63] and so, too, is the nominal DQ data (called a growth or "build up" curve). By a suitable alteration to the receiver phase of the experiment described above, one can measure signal that originates solely from the dynamics of the system. By "normalizing" the DQ build up data by this reference signal, which just comprises all remaining magnetization that has not evolved into DQ coherence, one can obtain a DQ signal that represents *solely* the structure of a given polymer melt, network, etc. Much work has been done by Saalwächter and coworkers on implementation, optimization, and artifacts associated with the MQ-NMR experiment, and the reader is referred to an excellent review article by Saalwächter and references therein.[63] The remainder of this chapter will instead

focus on the application of this technique towards understanding silicone elastomer materials.

Applications of MQ-NMR to Elastomeric Silicone Materials

While notable applications of MQ-NMR methodology have focused on melt-state polymers, more elegant studies have focused on elastomeric material, particularly with regards to understanding the effects of distributions and modalities of chain lengths, filler material, free chain ends, and other structural heterogeneities. For example, bimodal, end-linked PDMS networks were studied Saalwächter et al. in their 2003 work.[64] For a series of networks with variable short to long chain content, normalized DQ buildup curves were measured from which distributions of residual dipolar couplings were extracted. Obtaining these RDCs has been typically achieved by either fitting the build-up curves to an expression (yielding a single "average" RDC) or by employing more sophisticated regularization schemes (which are akin to inverse Laplace transform algorithms). These strategies use a kernel function using a *single* RDC to derive a *distribution* of RDCs that generally better fits the data. In the case of the bimodal PDMS networks, a clear bimodality of RDCs is observed post-regularization of the DQ build up data and the conclusions drawn from them – e.g. that long chains dynamics are not significantly affected by the presence of shorter chain lengths – are consistent with previous findings.[63]

Over the last 10 years, the kernel functions used to describe DQ build up curves have been refined and the calculated RDC distributions have consequently become more reliable.[53,54,63,89] Saalwächter and coworkers have applied these refined techniques to a wide variety of polymer phenomena such as gelation,

vulcanization, and swelling and have also extended significantly our knowledge of fundamental polymer physics, both confirming long standing scaling laws and calling into question some of the most basic assumptions of polymer statistical theory.[49,101-102]

Towards applications of silicone materials, there have been several elegant MQ-NMR studies. New materials often exploit or require exotic behavior from polymers and nanoporous fillers or membranes are popular for base polymer modification, tuning of properties, etc. For a series of PDMS/porous alumina membranes, Jagadeesh et al. demonstrated using MQ-NMR that several dynamically heterogeneous polymeric environments exist.[103] These populations were correlated to the degree to which chains are "intimate" or have knowledge of the nanoporous alumina surface. Extremely restricted PDMS chains ($D_{res} \sim 3.4$ kHz, vis-à-vis ~100 Hz for a melt) were detected and it was posited that this population of chains were uniaxially oriented at the nanopore surface.

In another study, Serbescu et al.[104] employed MQ-NMR to investigate solution blended, physical networks of PDMS and fumed silica. They determined that for native silica material, strong physical networks could be created. More interestingly, for surface modified silica material, a permanent, percolated network failed to form (due to the specifics of the modification) but 20-40% of the polymer formed a network-like material as determined from the NMR data. Notably, an aging study was also performed as part of this work demonstrating that over the course of many months, NMR revealed a significant increase in the network-like material of *mechanically* blended composite material. This result suggests long-

term morphological changes of the network topology and highlights solution blending as an "optimal" composite manufacturing strategy.

While the development of new polymeric materials is paramount to advancing various fields of application – medical, mechanical, aerospace, etc. – it is equally, if not more important to understand how these materials age within their service lifetimes. Engineering silicones are generally complex, multicomponent systems with many fillers, additives, etc. to precisely tune their mechanical resilience, thermal/chemical resistance, and reliable operation in a variety of other "harsh" environments. For the purposes of the remainder of this chapter, these improvements in the kernel now allow for the quantification of the distributions of molecular weights between physical and chemical constraints (and the use of swelling and/or variable temperature experiments can help distinguish between the two). The distributions in residual dipolar couplings obtained by MQ-NMR can be directly converted into a distribution of molecular weights of the network and any changes in this distribution can be quantified. This process is shown schematically in **Figure 18**.[105]

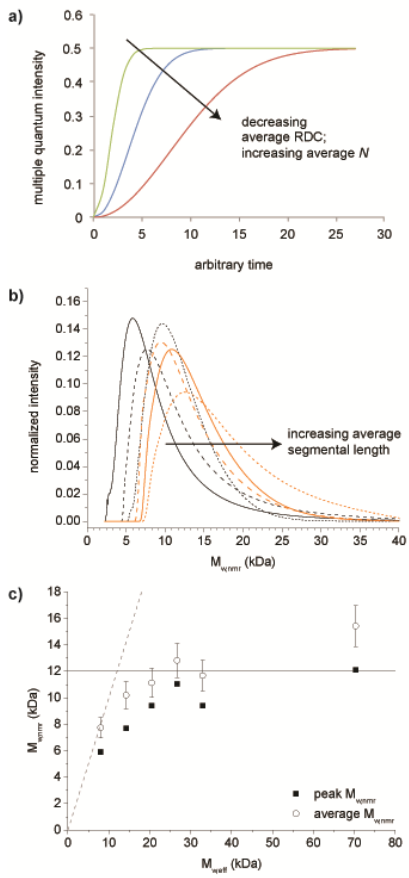

Figure 18. a) Generalized MQ-NMR build up curves. The arrow indicates build ups of increasingly weakly coupled systems with a lower average RDC. Regularization of these curves using a suitable kernel function can yield distributions of RDCs. b) Molecular weight distributions (MWDs) derived from the inverse relationship between D_{res} and both N and MWD for a series of bimodal PDMS networks with average parent chain MWD both above and below the entanglement limit, M_e. c) Peak and average molecular weights derived from the MWD in **Figure 17 (b)**. For networks with average molecular weight below M_e, the NMR-derived MWDs compare well with the stoichiometric network MWD average. For networks above M_e, entanglements dominate the NMR response and therefore there exists a plateau of molecular weight at roughly M_e.[105]

It has been well established by the authors and others[53,106-113] that exposure to ionizing radiation causes several interesting aging phenomena: decreases in elastic moduli at low dosages of gamma irradiation (< 100 kGy), reversal of this trend at high cumulative exposures, apparent silica/silicone interfacial desiccation,

among others. Understanding the roles and changes to elastomer network properties such as average and distributions of molecular weight, small molecule evolution, and competitions between chain scissioning and cross-linking are all critical to developing age aware models that seek to predict material performance with time. In articles by the authors, significant efforts have been made in understanding both model and engineering silicones, respectively.[105,111]

In a recent study,[105] model end-linked PDMS networks were synthesized over a range of molecular weights both below and above the melt entanglement limit and subsequently studied by MQ-NMR. Using basic assumptions they were able to convert RDC distributions into effective molecular weight distributions via

$$M_{w,NMR} = NC_{\infty}MW_{monomer} \propto D_{res}^{-1}. \qquad \textbf{(Equation 1.2)}$$

These NMR-derived molecular weight distributions were then used as the sole input to construct mesoscale computation models of end-linked networks. From these models, elastic moduli were computed and were them compared to dynamic mechanical analysis measurements. The researchers noted that under the current experimental conditions, the MQ-NMR data see physical entanglements as chemical cross links, predictions of elastic moduli are higher than measured values. Considering the bounds of network behavior as described through the affine and phantom models, they were able to estimate that the effect of treating these two constraints equally would results in an overestimation of elastic moduli by the computational approach by a factor of 3.2 to 6.8. Similar methodologies may be

employed as non-destructive techniques capable of monitoring relatively subtle changes in network structural motifs associated with material performance and degradation.

^{129}Xe NMR as a probe of Silicone Morphology and Degradation

It has been demonstrated that ^{129}Xe NMR is a sensitive spectroscopic probe to morphological changes in polymers.[114] Xenon is an ideal probe due to its high polarizability where xenon collisions with the walls of the polymer matrix distort the electron cloud surrounding the nucleus(polarize) manifesting as a change in the chemical shift in the ^{129}Xe spectrum.[115] The smaller the void structure, or the faster the chain motions, the higher the collisional frequency, and therefore the larger the observed chemical shift.[116] Such a high sensitivity of chemical shift to collisional frequency allows ^{129}Xe NMR to give complementary data to positron annihilation spectroscopy (PALS) when free volume measurements are sought.[117] In a recent study by the authors, the effect of compression set on void structure was investigated in fluorosilicone o-rings.[118] In this study, a complete elimination of void space was observed at the highest levels of compression (**Figure 19**). Without any additional room to compress, an o-ring will fail to maintain a seal. Studies such as these serve to demonstrate the utility of ^{129}Xe NMR techniques in the assessment of degradation and service lifetimes in complex silicones.

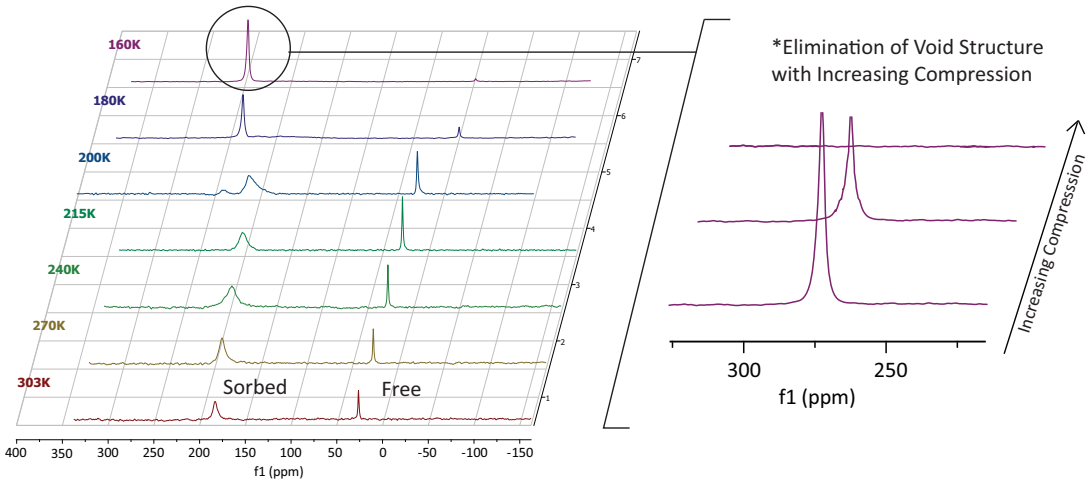

Figure 19. ^{129}Xe NMR spectra of a series of fluorosilicone elastomer o-rings that have been exposed to increasing levels of long term compressive force. The increasing loss of the 'free' Xe signal and the shifts in the sorbed Xe signal correlate clearly with a large reduction in void volume associated with the onset severe compression set.

Polymer blends that contain multiple morphological domains have with them distinct segmental motions. Consequently ^{129}Xe has been used to quantify ratios between crystalline and amorphous domains.[119]

Magnetic Resonance Imaging Techniques and their Application to Silicone Degradation

The advances in NMR methodologies previously described have successfully been used to characterize both chemical and morphological changes in silicone based materials. These techniques, however, excite indiscriminately giving a global average of the property changes in a material. Utilizing voxel selective techniques, MRI, allows for spatially selective excitation and detection of spin states thereby giving rise to a 3-dimensional map of NMR observables including: relaxation times, residual dipolar couplings D_{res}, and ∂D_{res}, as well as spin density. Multiple reviews of MRI methodology are available, including the reviews of MRI of elastomeric

materials by Blümler and Blumich and Callahan.[16-17] We refer those interested in experimental details are referred to these reviews. Here we review some recent applications.

The rich density of protons in silicone materials make spin density mapping the simplest use of MRI.[120] Shown here in **Figure 20** is a silicone foam pad manufactured with an extremely narrow distribution of pore sizes, having the dimensions of 1 x 1 x 0.2 cm with a well-defined pore spacing of 4 mm. When the pad is interrogated for its spin density an image of the network is obtained, (see b and c in **Figure 20**).

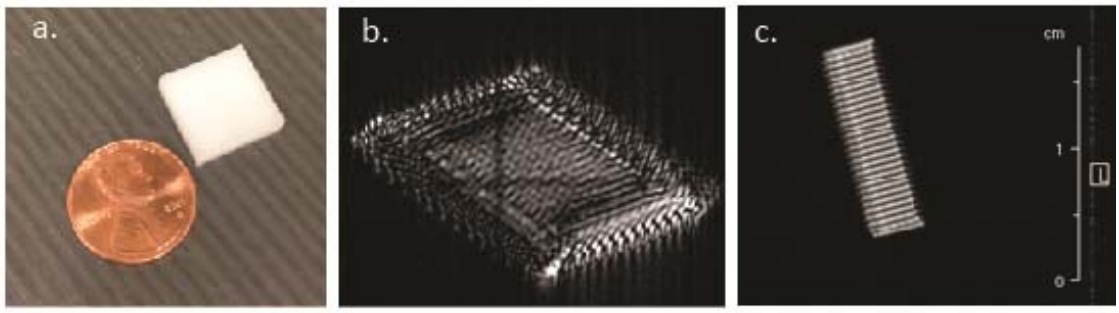

Figure 20. MRI imaging of silicone foam pad having a regular pore size (a). Though spatially resolved ^{1}H density spin mapping the structure of the manufactured part can be clearly imaged (b-c).

With a clear image of pore spacing, spin density mapping allows for a non-invasive means to assess pore structure and compression set. Depending on the size of filler particles, it is also possible to discriminate between polymer and filler in three dimensions as shown by Blumich[16] (see **Figure 21**).

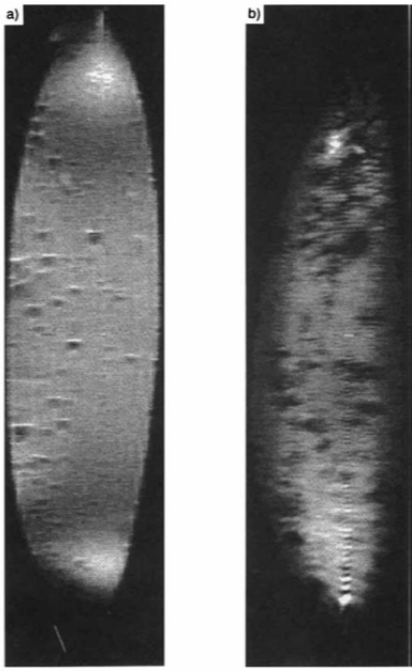

Figure 21. NMR images of a silicone rubber filled with silica obtained through two differing spatially resolved ^{1}H echo techniques. (a) Is a spin-echo image and (b) is a gradient echo derived image. Using both methods, agglomerations of silica filler particles (darker areas) are clearly visible.

As reviewed above, relaxation phenomena can be used to assess changes in segmental dynamics. Utilizing MRI methods that produce contrast (intensity) encoded with relaxation information provides an ability to measure dynamics in three dimensions on length scales of 10 to 100s of microns. One of the prominent forms of silicone aging is a change in the crosslink density manifests as a change in relaxation in the NMR observable. The CPMG echo technique is the simplest method to obtain T_2 contrast where the time between echoes, t, can be adjusted to optimize the contrast. T_2 contrast has been used to look at the effects of siloxane aging in a desiccating environment where a noticeable stiffening was observed.[121] In addition, radiation induced crosslinking[122] adds noticeably to the contrast in a T_2 mapped image, as shown in **Figure 22**. By combining the MSE with magnetic resonance

imaging (MRI), various studies have shown that it is possible to image even rigid components of silicone-based materials.[95]

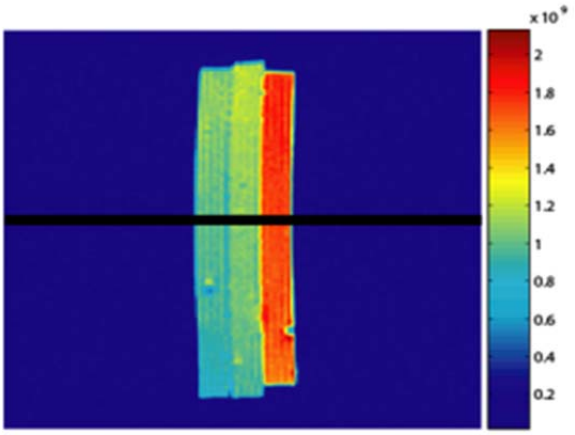

Figure 22. ^{1}H MRI of three DC745 elastomer pads exposed to increasing amounts of ionizing radiation [left to right: 0, 5, 25 MRad gamma cumulative dose]. The contrast is T_2 relaxation time obtained via spin-echo encoding.[123]

Relaxation weighted images have also been used to map out the effects of mechanical stress on silicone pads[123] (see **Figure 23**) and medical silicone implants.[124]

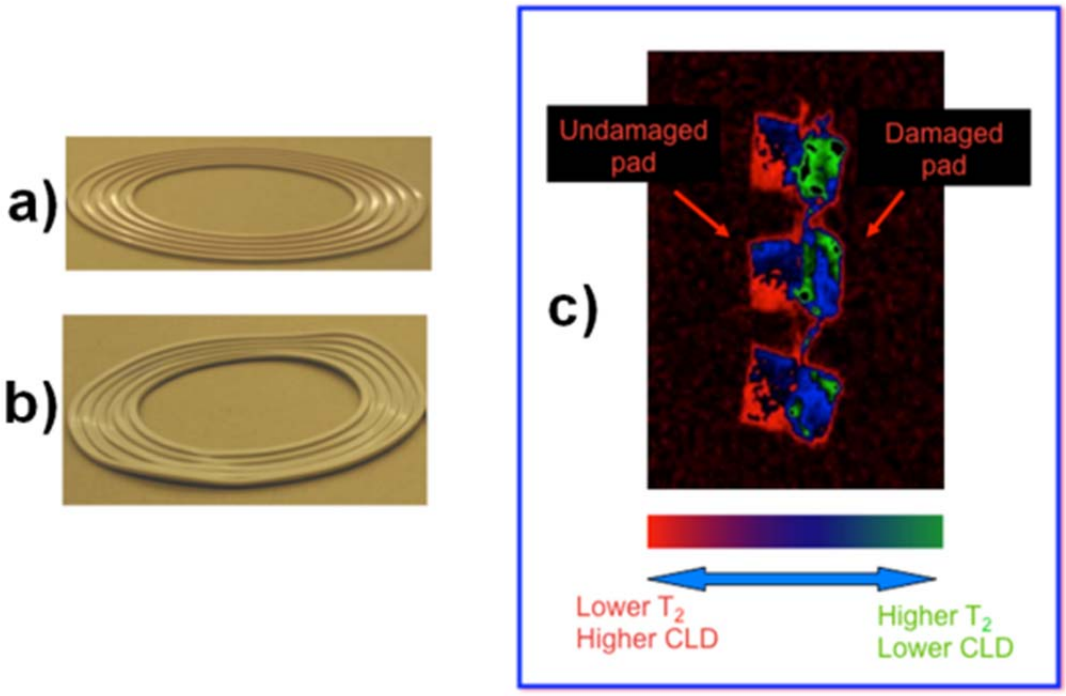

Figure 23. (a) pristine gasket formulated from DC745 commercial resin with solid peroxide specific curing agent; (b) gasket subjected to 50% compression for 15 years showing significant warp-age due to local areas of compression set; (c) T_2 contrast MRI of pads in (a) and (b) showing areas of lower crosslink density in the areas that exhibited significant compression set.[123]

Because of the widespread availability of MRI instrumentation in medical research laboratories and the amenability of MRI to the study of silicone polymers, it should not be surprising that the largest volume of literature on silicone MRI is that of silicone breast implants where significant contributions towards long term health and safety have been achieved.[18] Furthermore MRI based techniques are now heavily used in industry for quality control purposes where sudden changes in homogeneity are of concern.[16,124]

Use of NMR Data to Support Predictive Models of Silicone Networks

In recent years it has been demonstrated that NMR methodologies can be effectively utilized in the development and validation of predictive models of silicone networks. The information made available on a silicone network though the use of various NMR methodologies such as molecular weight distribution (MWD), effective crosslink density, modality, polymer-filler interactions and the presence of localized stresses, defects and inhomogeneities, can be used to both test and refine theoretical models which predict both network dynamics and degradation in silicone systems.

To illustrate the power of MQ-NMR, and its synergy with predictive modeling, a PDMS-based filled elastomeric rubber material (TR-55 from Dow Corning) was exposed to various dosages of γ radiation (Co-60 source (1.4MeV, 0.5Mrad/hour dose rate) in a non-reactive nitrogen atmosphere while being subjected to different strain levels λ_1. Following exposure to controlled duration (and therefore dosages) of radiation, each sample was removed from the irradiation chamber, released from the λ_1-strain, and allowed to relax at ambient conditions for a week. The relaxed samples were then subjected to two different sets of mechanical measurements:[112] (1) the new equilibrium length, called the recovered length λ_s, followed by (2) stress-strain analysis for strains of up to 50% elongation (using a TA Instruments ARES LS-2 rheometer in torsion rectangle geometry). The results of these measurements are summarized in **Figure 24**.

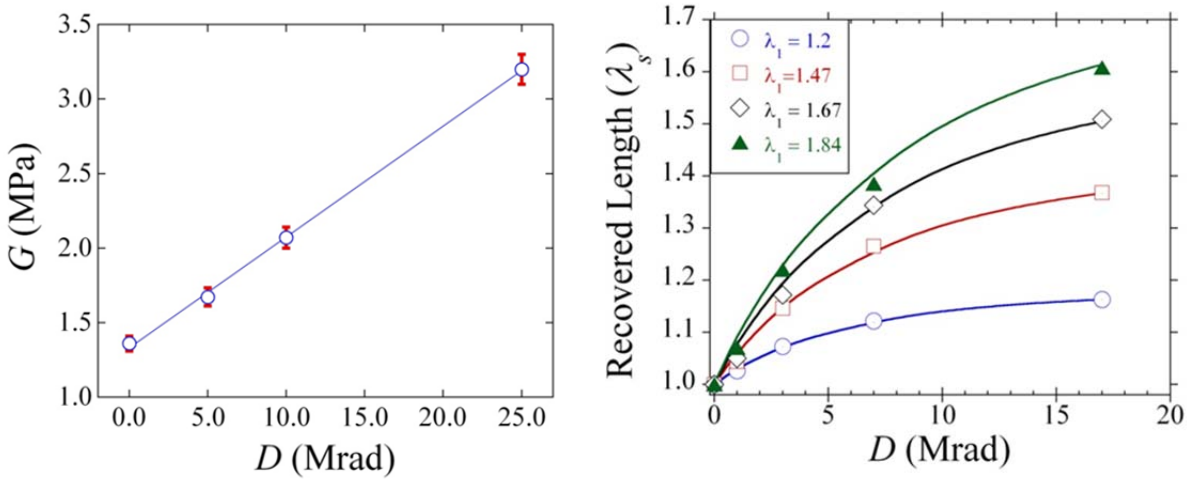

Figure 24. (Left) Measured shear modulus of TR-55 samples showing linear increase as a function of radiation dosage (D); (right) measured permanent set (expressed as recovered length λ_s) as a function of D for various strain levels (λ_1) at which the rubber samples were exposed to radiation.

The results of these two sets of measurements (**Figure 24**) can be cast in the form of two quantities that can be related to the evolution of MWD under radiation, i.e., new crosslinks created by radiation (f_{xl}) expressed as a fraction of the original network, and the fraction of the original network that gets modified (f_{mod}) in the process of creating new crosslinks. If the radiation exposure occurs under a state of strain (λ_1), then the net stress resulting from the network created by the new crosslinks and the modified original network is given by:[112,125-126]

$$\sigma(\lambda) = G_0\left\{(1-f_{\mathrm{mod}})(\lambda^2 - 1/\lambda) + f_{xl}(\lambda^2/\lambda_1^{\,2} - \lambda_1/\lambda)\right\} \quad , \qquad \textbf{(Equation 1.3)}$$

where σ represents true stress, G_0 the pristine shear modulus, and a neohookean materials response has been assumed.[127] From this model, the recovered length (λ_s) is given by:

$$\lambda_s = \left\{(1+f_{eff}\lambda_1)/(1+f_{eff}/\lambda_1^{\,2})\right\}^{1/3}, \qquad \text{where } f_{eff} = f_{xl}/(1\text{-}f_{mod}). \quad \textbf{(Equation 1.4)}$$

Several interesting results follow from the above analysis of **Figure 24**, including: (1) $f_{xl} - f_{mod} \propto D$, up to large radiation dosages; (2) for small D (< 5 Mrad) both f_{xl} and $f_{mod} \propto D$, and the ratio $f_{xl}/f_{mod} \sim 1.9$; (3) at higher D, the ratio f_{xl}/f_{mod} is nearly independent of the strain level λ_1. To obtain further insight, MQ-NMR was used to determine MWD of the rubber samples as a function of radiation dosage D.

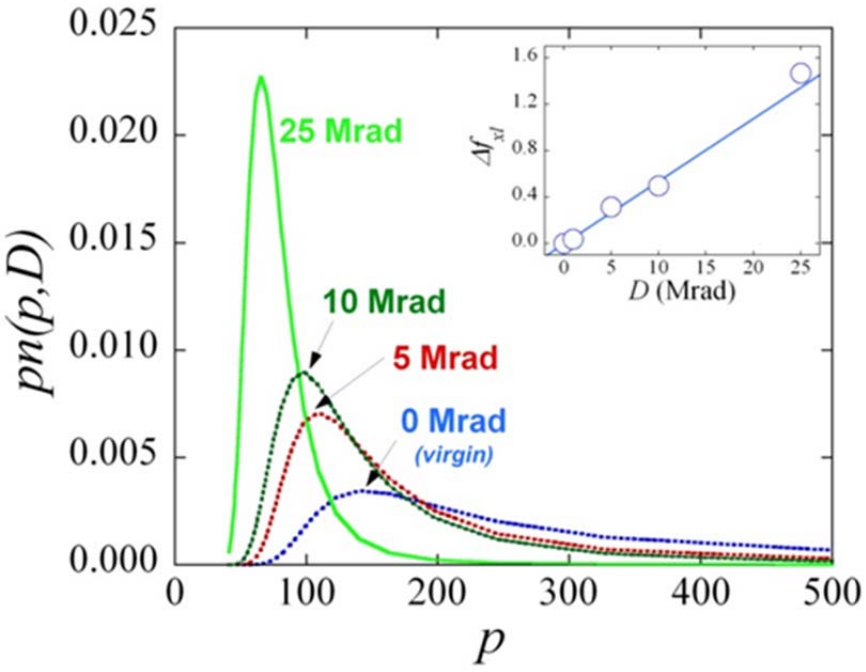

Figure 25. MWD ($pn(p,D)$) from MQ-NMR measurements for various radiation dosages. The data was interpreted by using N = 5.7 in Eq. (1.1). Inset: Corresponding chain density increment: $f_{xl} - f_{mod} = p_{av}(0)/p_{av}(D) - 1$ showing linear increase as a function of D.

Figure 25 displays the MQ-NMR spectra for the virgin material as well as for samples exposed to various radiation dosages. The intensity (y-axis) is proportional to the number of monomers in each chain-segment, i.e., $pn(p, D)$, where $n(p, D)$ is the frequency distribution of segments of length p monomers between successive crosslink junctions. The distribution in **Figure 25** represents the main MWD within the pure polymer part. In addition there is also a much weaker peak at smaller chain lengths (p <

20) that is likely associated with the silica fillers and/or resins inherent in the TR-55 formulation. Weak dipolar coupling at frequencies above 80 Hz can lead to significant uncertainties in the values of $n(p, D)$ at large values of p (> 300 or so), thus leading to uncertainty in the peak *heights* (especially for D ~ 10 Mrad or below). However, the peak *positions* are robust, as was verified through multiple measurements.[112] **Figure 25** displays a monotonic shift of the MWD to smaller chain lengths and gradual narrowing of the peak as a function of increasing radiation. More specifically, with increasing D the average chain length $p_{av}(D)$ decreases such that the crosslink density $f_{xl} - f_{mod} = p_{av}(0)/p_{av}(D) - 1$ increases linearly in the radiation dosage D.

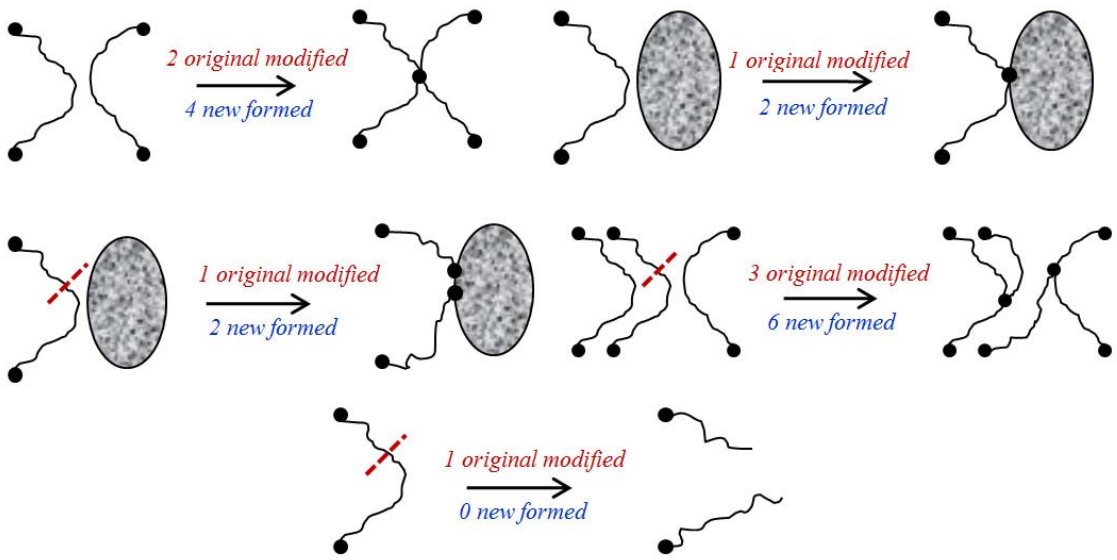

Figure 26. A schematic of how original chain modification and new crosslink formation can occur as a result of radiation-induced processes involving crosslinking (top two figures) and chain scission (bottom three figures). In all cases $f_{xl}/f_{mod} = 2$ except in the case where dangling chains form (bottom figure).

The above analysis does not identify the type of chemistry prevalent during radiation exposure: is it primarily the formation of new crosslinks, or is it chain scission

followed by crosslink formation? How would the results depend on the network functionality, i.e., three-fold or four-fold junctions? **Figure 26** schematically shows possible crosslinking and chain scission processes in a filled rubber that can be brought about by the energetic γ radiation. According to this schematic, except in the case of dangling bond formation, one should have $f_{xl}/f_{mod} \sim 2$. Thus, a value of $f_{xl}/f_{mod} \sim 1.9$ (as obtained above) indicates only a few percent of dangling bonds, but do not provide an indication of which of the various processes (in **Figure 26**) dominate. To address this question, the MWD results of **Figure 25** needed to be mimicked through simulations. Two different approaches were taken: (1) a coarse-grained mesoscale simulation approach[128] and (2) a statistical approach involving the population balance of chain lengths of crosslink segments.[113]

The mesoscale model consists of a set of crosslink nodes (i.e. junctions) connected via single finite extensible nonlinear elastic (FENE) bonds (that can be potentially crosslinked and/or scissioned), which represent the chain-segments between crosslinks. In addition, there is a repulsive Lennard-Jones interaction between all crosslink positions to simulate volume exclusion effects. The Lennard-Jones and FENE interaction parameters were adjusted and the degree of polymerization (p) for a given length of a FENE bond calibrated until the MWD computed from our network matched the experimental MWD of the virgin material.[112]

To simulate the radiation-induced evolution of the above network, the situation with only crosslinking and no scissioning was considered. Initially, a virgin network was constructed with only fourfold-connected junctions, and additional random crosslink operations between FENE bonds (i.e. segments) were performed.

New crosslinks were added in radiation dosage steps of 1 Mrad, and at each step the new network was structurally optimized (i.e. relaxed) using the LAMMPS code.[129] **Figure 27** displays the simulated evolution of MWD of the above network (red curve) under fourfold-coordination for four different radiation dosages along with the experimental data (blue line). The work also considered the MWD evolution when all new crosslinks were threefold-connected (i.e. scission-induced), as shown by green dashed lines. The differences in MWD between fourfold and three-fold connected cases turned out to be negligible, and both mechanisms led to excellent agreement in the peak positions as compared to NMR data.

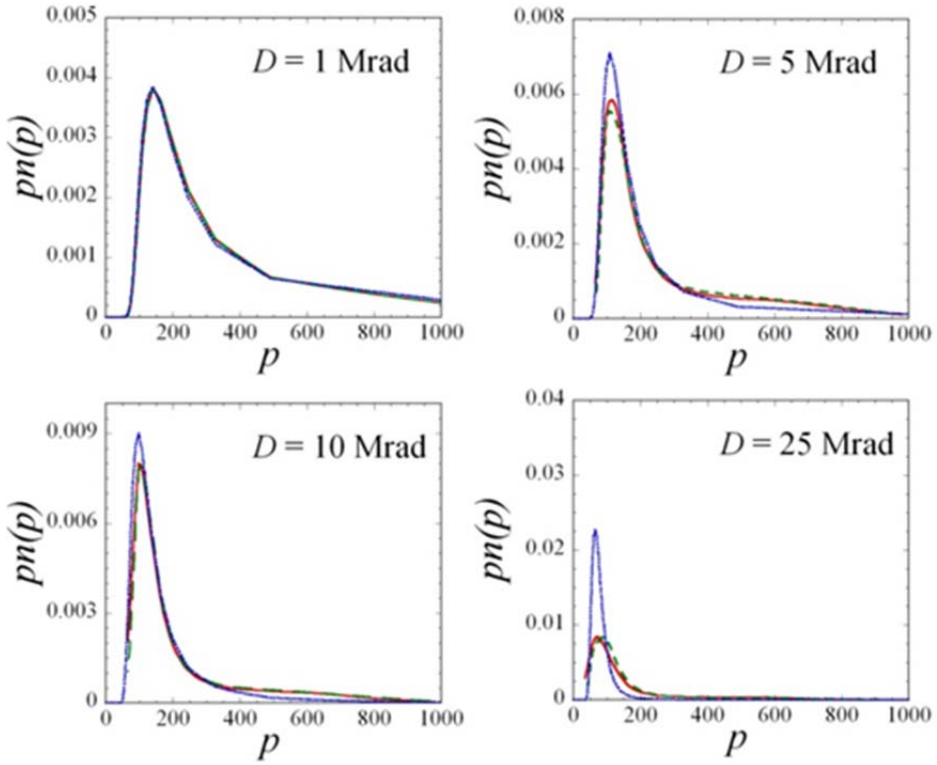

Figure 27. Comparison of experimental MWD of **Figure 25** (blue line) with computed MWD for fourfold-linking only (red solid line) and threefold-linking only (green dashed line).

The differences between peak heights, especially for $D \leq 10$ Mrad are not surprising given the uncertainty in the NMR data in the long-tail part. However at 25

Mrad, the disagreement between the experimental and simulated data is significant and point to effects not considered in the simulations. To explain such differences, simulations were performed allowing for the presence of dangling bonds (and/or loops) which did not form junctions. This led to simulated peaks to be narrower and higher, closer to the NMR data. Similar effects could also be expected from the creation of volatile small-chain fragments.

Finally, Dinh et al.[113] carried out a statistical analysis of the distribution of crosslink segment lengths and its evolution with network changes brought about by irradiation. The basic idea starts from the fact that when two chains of lengths p and q crosslink somewhere in the middle, it forms four chains of lengths $p - m$, m, $q - n$, and n (where $m < p$ and $n < q$). The evolution of the MWD, i.e., the frequency distribution of chains of different lengths is governed by the probabilities of different types of chemical processes caused by radiation, i.e., crosslinking, chain scissioning, loop formation, etc. It also depends upon the details of the type of crosslinking process, e.g., H-linking or Y-linking (see **Figure 28**) or a mixture of both.

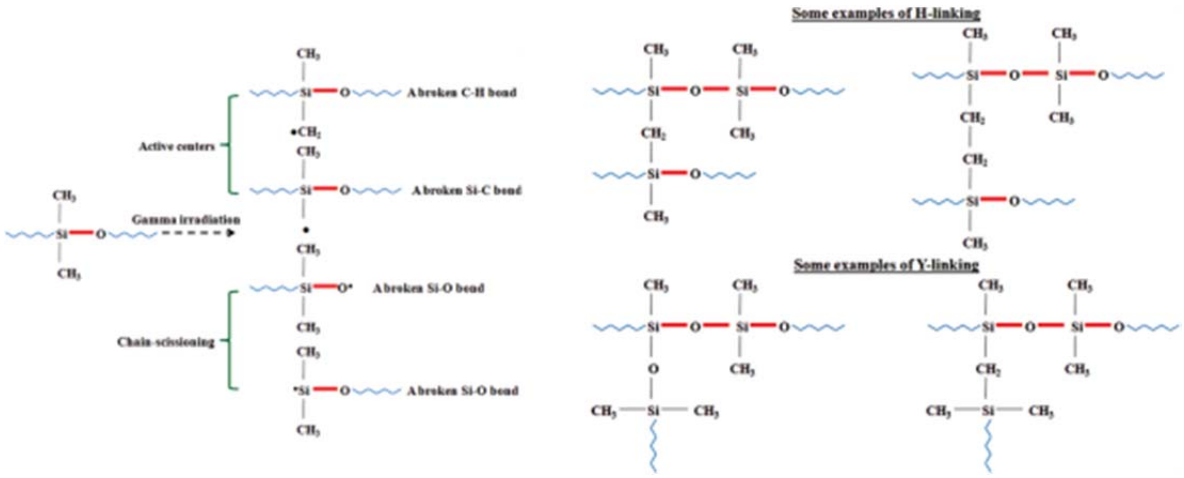

Figure 28. Left: Depiction of the active centers and chain-scissioning formed under gamma irradiation. Right: A schematic of possible structures formed via H-linking and Y-linking.

Such a method of tracking the distribution of chain lengths, known as population balance (PB) was first applied by Saito[130] to a set of initially free (i.e. non-crosslinked) polymer chains, while Dinh at al.[113] derived the PB equations appropriate for a system of crosslinked chains. The MQ-NMR MWD data on the virgin material (see **Figure 25**) was used to create a starting population of crosslink lengths, which was evolved according to various crosslinking and scissioning schemes. The hope was that by matching the simulated MWD evolution to the MQ-NMR data as a function of radiation one would be able to identify the dominant crosslinking scheme. Unfortunately, the PB-simulated MWD corresponding to several different crosslinking schemes were nearly identical, and agreement with the MQ-NMR was only qualitative in nature. Nonetheless, the work was able to put bounds on various rates of these processes and further confirmed that a competition of these phenomena determines the overall evolution of the effect of irradiation.

The results in this section demonstrate the utility of advanced NMR methodologies for the non-invasive and accurate characterization of silicone network properties. And when linked with effective modeling and simulations, NMR can provide novel insights into aging and degradation induced modifications occurring at the molecular level.

Conclusions

NMR is perhaps one of the most valuable and versatile tools for the study of complex Silicone elastomeric networks. Advanced multi-dimensional methodologies combined with isotopic enrichment now allow the both the elucidation of complex structures in silicones and the definitive determination of degradation mechanisms. MRI imaging provides spatial resolution of the chemical markers for aging and degradation. And in the broader study of structure-property relationships in complex silicone based materials NMR has much to offer. Techniques ranging from comparatively simple T_2 relaxometry through to advanced MQ-NMR and combined mesoscale modeling approaches continue to yield new insight into the links between the molecular architecture of silicone systems and their macroscopic properties. It is unsurprising then, that today it is NMR, despite its old moniker as 'the most insensitive spectroscopy' that stands alone in its ability to effectively probe the structure and properties of silicones from an atomistic to a macroscopic scale.

Acknowledgements

This work was performed under the auspices of the U.S. Department of Energy by Lawrence Livermore National Laboratory under Contract DE-AC52-07NA27344. The authors also gratefully acknowledge Sarah Chinn, Mogon Patel, Anthony Skinner, Anthony Swain, Todd Stephens, Tom Wilson, Ward Small, Cynthia Alviso, Todd Weisgraber, Harris Mason, Bryan Balazs, Mark Hoffman, Rick Gee, William Mclean II, and James LeMay for helpful discussions and support.

References

[1] R.L. Clough, N.C. Billingham, and K.T. Gillen, Polymer durability: Degradation, stabilization, and lifetime prediction, in: Advances in Chemistry Series, American Chemical Society, New York, pp. 728, 1996.
[2] K.T. Gillen, J. Wise, and R.L. Clough, *Polymer Degradation and Stability*, Vol. 47, 149-161, 1995.
[3] P. Denner, L. Deutschbein, and B. Walter, *Journal of Macromolecular Science-Physics*, Vol. B38, 1023-1035, 1999.
[4] T.M. Alam, M. Celina, R.A. Assink, R.L. Clough, K.T. Gillen, and D.R. Wheeler, *Macromolecules*, Vol. 33, 1181-1190, 2000.
[5] D. Campbell, R. Pethrick, and J.R. White, *Polymer Characterization: Physical Techniques*, 2 ed., Stanley Thornes, Cheltenham, UK, 2000.
[6] J.H. Kinney, G.W. Marshall, S.J. Marshall, and D.L. Haupt, *Journal of Applied Polymer Science*, Vol. 80, 1746-1755, 2001.
[7] B.M. Patterson, K. Henderson, and Z. Smith, *Journal of Materials Science*, Vol. 48, 1986-1996, 2013.
[8] P.R. Morrell, M. Patel, and S. Pitts, *Polymer Testing*, Vol. 31, 102-109, 2012.
[9] J.P. Lewicki, J.J. Liggat, R.A. Pethrick, M. Patel, and I. Rhoney, *Polymer Degradation and Stability*, Vol. 93, 158-168, 2008.
[10] L. Jayes, A.P. Hard, C. Sene, S.F. Parker, and U.A. Jayasooriya, *Analytical Chemistry*, Vol. 75, 742-746, 2003.
[11] V. Arrighi, S. Gagliardi, A.C. Dagger, J.A. Semlyen, J.S. Higgins, and M.J. Shenton, *Macromolecules*, Vol. 37, 8057-8065, 2004.
[12] K. Schmidt-Rohr, and H.W. Spiess, *Multidimensional Solid-State NMR and Polymers*, 1 ed., Academic Press, San Diego, California, 1994.
[13] T. Asakura, and I. Ando, *Solid State NMR of Polymers*, 1 ed., Elsevier Science B.V., Amsterdam, The Netherlands, 1998.
[14] F. Bovey, and P.A. Mirau, *NMR of Polymers*, Academic Press Inc., London, UK, 455, 1996.
[15] K.J.D. MacKenzie, and M.E. Smith, *Multinuclear Solid-State Nuclear Magnetic Resonance of Inorganic Materials*, Elsevier Science Ltd., Oxford, UK, 2002.
[16] P. Blumler, and B. Blumich, *Rubber Chemistry and Technology*, Vol. 70, 468-518, 1997.
[17] P.T. Callaghan, *Principles of Nuclear Magnetic Resonance Microscopy*, Oxford University Press, Oxford, UK, 1994.
[18] S. Stinson, *Chemical & Engineering News*, Vol. 70, 27-27, 1992.
[19] M.A. Brook, *Silicon in Organic, Organometallic and Polymer Chemistry*, John Wiley and Sons Inc., New York, US, 1999.
[20] R.K. Harris, and B.J. Kimber, *Applied Spectroscopy Reviews*, Vol. 10, 117-137, 1975.
[21] A.L. Smith, The Analytical Chemistry of Silicones, in: J.D. Winefordner (Ed.) Chemical Analysis: A Series of Monographs on Analytical Chemistry and Its Applications, Academic Press inc., San Diego, CA, US, pp. 455.
[22] K. Beshah, J.E. Mark, J.L. Ackerman, and A. Himstedt, *Journal of Polymer Science*

Part B-Polymer Physics, Vol. 24, 1207-1225, 1986.
[23] A. Labouriau, J.D. Cox, J.R. Schoonover, B.M. Patterson, G.J. Havrilla, T. Stephens, and D. Taylor, *Polymer Degradation and Stability*, Vol. 92, 414-424, 2007.
[24] A.B. Birkefeld, R. Bertermann, H. Eckert, and B. Pfleiderer, *Biomaterials*, Vol. 24, 35-46, 2003.
[25] T.M. Alam, M. Celina, R.A. Assink, R.L. Clough, and K.T. Gillen, *Radiation Physics and Chemistry*, Vol. 60, 121-127, 2001.
[26] T.M. Alam, *Radiation Physics and Chemistry*, Vol. 62, 145-152, 2001.
[27] T.M. Alam, *Abstracts of Papers of the American Chemical Society*, Vol. 221, U343-U343, 2001.
[28] J.M. Skutnik, R.A. Assink, and M. Celina, *Polymer*, Vol. 45, 7463-7469, 2004.
[29] A. Abragam, *The Principles of Nuclear Magnetism A. Abragam*, Oxford University Press, Oxford, UK, 2006.
[30] C.P. Slichter, *Principles of Magnetic Resonance*, 3 ed., Springer, New York, 1996.
[31] G.E. Maciel, "Siloxane-Based Solid Networks, from Silicas to Silicones." In: J.J. Fitzgerald, ed., *Solid-State NMR Spectroscopy of Inorganic Materials*, American Chemical Society, pp. 326-56, 1999.
[32] A. Labouriau, D. Taylor, T.S. Stephens, and M. Pasternak, *Polymer Degradation and Stability*, Vol. 91, 1896-1902, 2006.
[33] Chemical Speciation and Network Dynamics in Well-Defined Model Silicone Network Elastomers, Lawrence Livermore National Laboratory, Livermore, CA, 2012.
[34] M. Patel, P. Morrell, J. Cunningham, N. Khan, R.S. Maxwell, and S.C. Chinn, *Polymer Degradation and Stability*, Vol. 93, 513-519, 2008.
[35] R.A. Fry, N. Tsomaia, C.G. Pantano, and K.T. Mueller, *Journal of the American Chemical Society*, Vol. 125, 2378-2379, 2003.
[36] J.P. Cohenaddad, P. Huchot, P. Jost, and A. Pouchelon, *Polymer*, Vol. 30, 143-146, 1989.
[37] R.H. Ebengou, and J.P. Cohenaddad, *Polymer*, Vol. 35, 2962-2969, 1994.
[38] J.P. Cohenaddad, and A. Viallat, *Polymer*, Vol. 27, 1855-1863, 1986.
[39] A. Viallat, J.P. Cohenaddad, and A. Pouchelon, *Polymer*, Vol. 27, 843-848, 1986.
[40] J.P. Cohen Addad, *Physical Properties of Polymeric Gels*, John Wiley and Sons, New York, 1996.
[41] A. Charlesby, *Nature*, Vol. 173, 679-680, 1954.
[42] R. Folland, and A. Charlesby, *International Journal for Radiation Physics and Chemistry*, Vol. 8, 555-562, 1976.
[43] R. Folland, and A. Charlesby, *Radiation Physics and Chemistry*, Vol. 10, 61-68, 1977.
[44] A. Charlesby, *Radiation Physics and Chemistry*, Vol. 39, 45-51, 1992.
[45] A.A. Parker, J.J. Marcinko, Y.T. Shieh, D.P. Hedrick, and W.M. Ritchey, *Journal of Applied Polymer Science*, Vol. 40, 1717-1725, 1990.
[46] R. Guyonnet, and J.P. Cohenaddad, *Macromolecules*, Vol. 22, 135-142, 1989.
[47] J.P. Cohenaddad, *Macromolecules*, Vol. 22, 147-151, 1989.
[48] W. Gronski, U. Hoffmann, G. Simon, A. Wutzler, and E. Straube, *Rubber Chemistry and Technology*, Vol. 65, 63-77, 1992.
[49] K. Saalwächter, and D. Reichert, "Magnetic Resonance: Polymer Applications of

NMR", in: J. Lindon, G. Tranter, and D. Koppenaal, eds., *Encyclopedia of Spectroscopy & Spectrometry*, Elsevier, Oxford, UK, pp. 2221-2236, 2010.
[50] M.G. Brereton, *Macromolecules*, Vol. 23, 1119-1131, 1990.
[51] D.A. Vega, M.A. Villar, E.M. Valles, C.A. Steren, and G.A. Monti, *Macromolecules*, Vol. 34, 283-288, 2001.
[52] A.K. Whittaker, T. Bremner, and F.O. Zelaya, *Polymer*, Vol. 36, 2159-2164, 1995.
[53] S.C. Chinn, C.T. Alviso, E.S.F. Berman, C.A. Harvey, R.S. Maxwell, T.S. Wilson, R. Cohenour, K. Saalwächter, and W. Chasse, *Journal of Physical Chemistry B*, Vol. 114, 9729-9736, 2010.
[54] W. Chasse, J.L. Valentin, G.D. Genesky, C. Cohen, and K. Saalwächter, *Journal of Chemical Physics*, Vol. 134, 2011.
[55] M. Garbarczyk, F. Grinberg, N. Nestle, and W. Kuhn, *Journal of Polymer Science Part B-Polymer Physics*, Vol. 39, 2207-2216, 2001.
[56] Papon, K. Saalwächter, K. Schaler, L. Guy, F. Lequeux, and H. Montes, *Macromolecules*, Vol. 44, 913-922, 2011.
[57] D.E. Demco, and B. Blumich, *Current Opinion in Solid State & Materials Science*, Vol. 5, 195-202, 2001.
[58] A. Papon, H. Montes, F. Lequeux, J. Oberdisse, K. Saalwächter, and L. Guy, *Soft Matter*, Vol. 8, 4090-4096, 2012.
[59] R.C. Ball, P.T. Callaghan, and E.T. Samulski, *Journal of Chemical Physics*, Vol. 106, 7352-7361, 1997.
[60] P.T. Callaghan, and E.T. Samulski, *Macromolecules*, Vol. 30, 113-122, 1997.
[61] R.S. Maxwell, and B. Balazs, *Nuclear Instruments & Methods in Physics Research Section B-Beam Interactions with Materials and Atoms*, Vol. 208, 199-203, 2003.
[62] P. Sotta, and B. Deloche, *Macromolecules*, Vol. 23, 1999-2007, 1990.
[63] K. Saalwächter, *Progress in Nuclear Magnetic Resonance Spectroscopy*, Vol. 51, 1-35, 2007.
[64] K. Saalwächter, P. Ziegler, O. Spyckerelle, B. Haidar, A. Vidal, and J.U. Sommer, *Journal of Chemical Physics*, Vol. 119, 3468-3482, 2003.
[65] F.V. Chavez, and K. Saalwächter, *Macromolecules*, Vol. 44, 1549-1559, 2011.
[66] R.S. Maxwell, R.H. Gee, T. Baumann, N. Lacevic, J.L. Herberg, and S.C. Chinn, *Advances in Silicones and Silicone-Modified Materials*, Vol. 1051, 75-84, 2010.
[67] W. Chasse, M. Lang, J.U. Sommer, and K. Saalwächter, *Macromolecules*, Vol. 45, 899-912, 2012.
[68] R.R. Ernst, G. Bodenhausen, and A. Wokaun, *Prinicples of Nuclear Magnetic Resonance in One and Two Dimensions*, Oxford University Press, Oxford, UK, 2004.
[69] P. Pelupessy, L. Duma, and G. Bodenhausen, *Journal of Magnetic Resonance*, Vol. 194, 169-174, 2008.
[70] J. Weber, P. Rosch, K. Adermann, W.G. Forssmann, and A. Wokaun, *Biochim. Biophys. Acta-Protein Struct. Molec. Enzym.*, Vol. 1207, 231-235, 1994.
[71] M.H. Chai, Z.J. Pi, C. Tessier, and P.L. Rinaldi, *Journal of the American Chemical Society*, Vol. 121, 273-279, 1999.
[72] W.X. Liu, P.L. Rinaldi, L. Galya, J.E. Hansen, and L. Wilczek, *Organometallics*, Vol. 21, 3250-3257, 2002.
[73] O.B. Peersen, X.L. Wu, I. Kustanovich, and S.O. Smith, *Journal of Magnetic Resonance Series A*, Vol. 104, 334-339, 1993.

[74] M. Hetem, G. Rutten, L. Vandeven, J. Dehaan, and C. Cramers, *Journal of High Resolution Chromatography & Chromatography Communications*, Vol. 11, 510-516, 1988.
[75] P. Conte, R. Spaccini, and A. Piccolo, *Analytical and Bioanalytical Chemistry*, Vol. 386, 382-390, 2006.
[76] C.T.M. Fransen, H. van Laar, J.P. Kamerling, and J.F.G. Vliegenthart, *Carbohydrate Research*, Vol. 328, 549-559, 2000.
[77] G.E. Maciel, and D.W. Sindorf, *Journal of the American Chemical Society*, Vol. 102, 7606-7607, 1980.
[78] D.W. Sindorf, and G.E. Maciel, *Journal of the American Chemical Society*, Vol. 105, 1487-1493, 1983.
[79] D.W. Sindorf, and G.E. Maciel, *Journal of the American Chemical Society*, Vol. 105, 3767-3776, 1983.
[80] M. Aramata, and T. Igarashi, *Bunseki Kagaku*, Vol. 47, 971-978, 1998.
[81] F. Milanesi, G. Cappelletti, R. Annunziata, C.L. Bianchi, D. Meroni, and S. Ardizzone, *Journal of Physical Chemistry C*, Vol. 114, 8287-8293, 2010.
[82] R. Luliucci, C. Taylor, and W.K. Hollis, *Magnetic Resonance in Chemistry*, Vol. 44, 375-384, 2006.
[83] D.E. Demco, R. Fechete, and B. Blumich, *Chemical Physics Letters*, Vol. 375, 406-412, 2003.
[84] M. Bertmer, M.F. Wang, D.E. Demco, and B. Blumich, *Solid State Nuclear Magnetic Resonance*, Vol. 30, 45-54, 2006.
[85] B. Jagadeesh, D.E. Demco, and B. Blumich, *Chemical Physics Letters*, Vol. 393, 416-420, 2004.
[86] M.F. Wang, M. Bertmer, D.E. Demco, B. Blumich, V.M. Litvinov, and H. Barthel, *Macromolecules*, Vol. 36, 4411-4413, 2003.
[87] V.M. Kenkre, E. Fukushima, and D. Sheltraw, *Journal of Magnetic Resonance*, Vol. 128, 62-69, 1997.
[88] J. Lapham, J.P. Rife, P.B. Moore, and D.M. Crothers, *Journal of Biomolecular Nmr*, Vol. 10, 255-262, 1997.
[89] S. Chinn, S. DeTeresa, A. Sawvel, A. Shields, B. Balazs, and R.S. Maxwell, *Polymer Degradation and Stability*, Vol. 91, 555-564, 2006.
[90] N.M. Lacevic, R.S. Maxwell, A. Saab, and R.H. Gee, *Journal of Physical Chemistry B*, Vol. 110, 3588-3594, 2006.
[91] J.L. Valentin, D. Lopez, R. Hernandez, C. Mijangos, and K. Saalwächter, *Macromolecules*, Vol. 42, 263-272, 2009.
[92] M. Kovermann, K. Saalwächter, and W. Chasse, *Journal of Physical Chemistry B*, Vol. 116, 7566-7574, 2012.
[93] S.C. Chinn, A. Cook-Tendulkar, R. Maxwell, H. Wheeler, M. Wilson, and Z.H. Xie, *Polymer Testing*, Vol. 26, 1015-1024, 2007.
[94] M. Kruger, A. Schwarz, and B. Blumich, *Magnetic Resonance Imaging*, Vol. 25, 215-218, 2007.
[95] B. Blumich, *NMR Imaging of Materials*, Oxford University Press, Oxford, UK, 2000.
[96] S. Valic, P. Sotta, and B. Deloche, *Polymer*, Vol. 40, 989-994, 1999.
[97] P. Sotta, *Macromolecules*, Vol. 31, 3872-3879, 1998.

[98] P. Sotta, and B. Deloche, *Journal of Chemical Physics*, Vol. 100, 4591-4600, 1994.
[99] P. Sotta, B. Deloche, J. Herz, A. Lapp, D. Durand, and J.C. Rabadeux, *Macromolecules*, Vol. 20, 2769-2774, 1987.
[100] B. Deloche, and E.T. Samulski, *Macromolecules*, Vol. 14, 575-581, 1981.
[101] K. Saalwächter, *Journal of the American Chemical Society*, Vol. 125, 14684-14685, 2003.
[102] A. Krushelnitsky, E. deAzevedo, R. Linser, B. Reif, K. Saalwächter, and D. Reichert, *Journal of the American Chemical Society*, Vol. 131, 12097-12099, 2009.
[103] A. Buda, D.E. Demco, B. Jagadeesh, and B. Blumich, *Journal of Chemical Physics*, Vol. 122, 2005.
[104] A. Serbescu, and K. Saalwächter, *Polymer*, Vol. 50, 5434-5442, 2009.
[105] B.P. Mayer, J.P. Lewicki, T.H. Weisgraber, W. Small, S.C. Chinn, and R.S. Maxwell, *Macromolecules*, Vol. 44, 8106-8115, 2011.
[106] D.J.T. Hill, C.M.L. Preston, and A.K. Whittaker, *Polymer*, Vol. 43, 1051-1059, 2002.
[107] R.S. Maxwell, and B. Balazs, *Journal of Chemical Physics*, Vol. 116, 10492-10502, 2002.
[108] R.S. Maxwell, S.C. Chinn, D. Solyom, and R. Cohenour, *Macromolecules*, Vol. 38, 7026-7032, 2005.
[109] M. Patel, A.C. Swain, J.L. Cunningham, R.S. Maxwell, and S.C. Chinn, *Polymer Degradation and Stability*, Vol. 91, 548-554, 2006.
[110] A. Maiti, R.H. Gee, T. Weisgraber, S. Chinn, and R.S. Maxwell, *Polymer Degradation and Stability*, Vol. 93, 2226-2229, 2008.
[111] B.P. Mayer, S.C. Chinn, R.S. Maxwell, and J.A. Reimer, *Chemical Engineering Science*, Vol. 64, 4684-4692, 2009.
[112] A. Maiti, T. Weisgraber, L.N. Dinh, R.H. Gee, T. Wilson, S. Chinn, and R.S. Maxwell, *Physical Review E*, Vol. 83, 2011.
[113] L.N. Dinh, B.P. Mayer, A. Maiti, S.C. Chinn, and R.S. Maxwell, *Journal of Applied Physics*, Vol. 109, 2011.
[114] J.B. Miller, *Rubber Chemistry and Technology*, Vol. 66, 455-461, 1993.
[115] J.B. Miller, J.H. Walton, and C.M. Roland, *Macromolecules*, Vol. 26, 5602-5610, 1993.
[116] H. Omi, T. Ueda, N. Kato, K. Miyakubo, and T. Eguchi, *Physical Chemistry Chemical Physics*, Vol. 8, 3857-3866, 2006.
[117] T.C. Merkel, L.G. Toy, A.L. Andrady, H. Gracz, and E.O. Stejskal, *Macromolecules*, Vol. 36, 353-358, 2003.
[118] S.J. Harley, B.P. Mayer, E.A. Glascoe, R.S. Maxwell, G. White, and R. Bernstien, *Polymer Degradation and Stability*, Vol., in preparation.
[119] J.H. Walton, J.B. Miller, and C.M. Roland, *Journal of Polymer Science Part B-Polymer Physics*, Vol. 30, 527-532, 1992.
[120] L. Garrido, J.L. Ackerman, J.M. Vevea, J.E. Mark, and S.H. Wang, *Polymer*, Vol. 33, 1826-1830, 1992.
[121] B.R. Cherry, and T.M. Alam, *Polymer*, Vol. 45, 5611-5618, 2004.
[122] A. Chien, R. Maxwell, D. Chambers, B. Balazs, and J. LeMay, *Radiation Physics and Chemistry*, Vol. 59, 493-500, 2000.
[123] J.L. Herberg, S.C. Chinn, A.M. Sawvel, E. Gjersing, and R.S. Maxwell, *Polymer*

Degradation and Stability, Vol. 91, 1701-1710, 2006.
[124] E.W. Abel, K.I. Wheeler, J.A. Chudek, G. Hunter, and F.M. Som, *Biomaterials*, Vol. 19, 55-60, 1998.
[125] A.V. Tobolsky, I.B. Prettyman, and J.H. Dillon, *Journal of Applied Physics*, Vol. 15, 380-395, 1944.
[126] R.D. Andrews, A.V. Tobolsky, and E.E. Hanson, *Journal of Applied Physics*, Vol. 17, 352-361, 1946.
[127] L.R.G. Treloar, *The Physics of Rubber Elasticity*, Clarendon Press, Oxford, UK, 1975.
[128] T.H. Weisgraber, R.H. Gee, A. Maiti, D.S. Clague, S. Chinn, and R.S. Maxwell, *Polymer*, Vol. 50, 5613-5617, 2009.
[129] S.N. Laboratories, LAMMPS Molecular Dynamics Simulator, 2004.
[130] O. Saito, *Journal of the Physical Society of Japan*, Vol. 13, 198-206, 1958.